Département de géomatique appliquée
Faculté des lettres et sciences humaines
Université de Sherbrooke

Développement d'une méthode de télédétection pour l'identification d'espèces exotiques envahissantes dans l'agglomération de Québec

NININAHAZWE Fiston

Mémoire présenté pour l'obtention du grade de Maître ès sciences géographiques (M.Sc.), cheminement de type recherche en Géomatique appliquée

Septembre 2022

Composition du jury

Directeur de recherche : Jérôme Théau

Professeur, Département de géomatique appliquée, Faculté des lettres et sciences humaines, Université de Sherbrooke.

Co-directeur de recherche : Mathieu Varin

Chef du Laboratoire de télédétection, Centre d'enseignement et de recherche en foresterie (CERFO).

Membre du jury interne : Kalifa Goïta

Professeur, Département de géomatique appliquée, Faculté des lettres et sciences humaines, Université de Sherbrooke.

Membre du jury externe : Saeid Homayouni

Professeur, Institut national de la recherche scientifique et Professeur associé, Laboratoire de télédétection environnementale et nordique.

Résumé

Les espèces exotiques envahissantes végétales (EEEv) sont actuellement considérées comme étant à l'origine de plusieurs types d'impacts négatifs dont la perte de la biodiversité et l'altération du fonctionnement des écosystèmes. Dans l'agglomération de Québec, la présence de plusieurs EEEv et les informations partielles sur leur distribution territoriale limitent la mise en place de stratégies efficaces de contrôle et d'éradication. Ces données sur la distribution territoriale peuvent être acquises à partir des inventaires *in situ.* Cependant, ces derniers nécessitent beaucoup de temps surtout dans les milieux envahis par plusieurs EEEv en même temps tels que les milieux urbains. Ces inventaires ne sont également pas adaptés financièrement et techniquement, lorsqu'il s'agit de grandes étendues ou lorsque les conditions topographiques ne sont pas favorables. La télédétection pourrait être utilisée pour contrer ces limites afin de cartographier les EEEv, suivre leur prolifération et intervenir rapidement. Le but de cette étude consistait donc à élaborer une méthode de cartographie multi-espèces par télédétection de cinq EEEv terrestres présentes dans l'agglomération de Québec, à savoir la renouée du Japon (*Fallopia japonica*), le phragmite (*Phragmites australis*), la berce du Caucase (*Heracleum mantegazzianum*), le nerprun bourdaine (*Frangula alnus)* et le nerprun cathartique (*Rhamnus cathartica*). L'approche méthodologique consistait à réaliser une cartographie mono-date et multi-date à l'aide d'images satellitaires WorldView-3 acquises en été, SPOT-7 et GeoEye-1 acquises en automne. Une classification orientée-objet combinée à des méthodes d'apprentissage automatique non paramétriques, à savoir *Support Vector Machine* (SVM), *Random Forest* (RF) et *Extreme Gradient Boosting* (XGBoost) a été utilisée afin de produire des probabilités de présence de ces EEEv. La cartographie des nerpruns a été réalisée à part car leur faible présence sur la zone d'étude et leur distribution sous-couvert à faible densité a nécessité un ajout de l'image GeoEye-1 et un paramétrage des méthodes différent de celui utilisé pour les trois premières EEEv. La combinaison des images WorldView-3 et SPOT-7 a permis d'atteindre d'excellentes performances pour les trois premières EEEv, avec un coefficient Kappa de 0,85 et une précision globale de 91 % en utilisant RF. Les performances individuelles des classes basées sur l'indicateur F1-score ont montré que la renouée du Japon est mieux détectée (F1-score maximal = 0,95), que la berce du Caucase (F1-score maximal = 0,91) et le phragmite (F1-score maximal = 0,87). La classification

multi-date des nerpruns est, par contre, moins performante par rapport à celle des autres espèces avec un coefficient Kappa égal à 0,72, une précision globale de 83 % et F1-score maximal égal 0,62. Cette étude montre la possibilité de cartographie et suivi des principales EEEv selon une approche multi-date. Les limites de cette étude, à savoir la faible quantité de données de référence d'EEEv, les coûts élevés d'acquisition et la faible disponibilité des images satellitaires à très haute résolution spatiale ainsi que la distribution des nerpruns en sous-couvert (dans notre zone d'étude) pourraient être réduites en utilisant des images plus accessibles en combinaison avec les techniques de super-résolution. Les données LiDAR à haute densité pourraient également être intégrées à l'imagerie optique afin d'améliorer les performances de cartographie des nerpruns.

Mots clés : Cartographie, espèces exotiques envahissantes, imagerie multispectrale, classification multi-date par analyse orientée-objet, apprentissage automatique.

Table des Matières

Liste des figures

Liste des tableaux

Liste des annexes

Avant-propos

Trois parties principales constituent l'essentiel de ce mémoire. La première partie met en contexte l'étude réalisée et présente les objectifs de travail. La deuxième partie est constituée de deux manuscrits d'articles scientifiques. Le premier manuscrit dont le titre est *« Mapping invasive alien plant species with very high spatial resolution and multi-date satellite imagery using object-based and machine learning techniques: A comparative study »* a été soumis le 04 Août 2022 au journal scientifique *GIScience & Remote Sensing*. Le titre du deuxième manuscrit est *« Mapping common and glossy buckthorns (Frangula alnus and Rhamnus cathartica) using multi-date satellite imagery WorldView-3, GeoEye-1 and SPOT-7»* et a été soumis au journal scientifique *International Journal of Digital Earth* le 08 Août 2022. La preuve de soumission de ces manuscrits est présentée à l'annexe 1 et 2, respectivement.

La troisième partie du mémoire présente une discussion générale des résultats obtenus et une conclusion générale qui mentionnent les principaux apports du projet, les limites rencontrées et perspectives pour les projets futurs.

Remerciements

Ce travail est le résultat d'un long parcours, le chemin n'a pas été un long fleuve tranquille et c'est pour cette raison que je profite de cette occasion afin de remercier toute personne qui, de près ou de loin, a apporté son soutien à sa réalisation. Je remercie profondément et sincèrement le professeur Jérôme Théau, mon directeur de recherche et M. Mathieu Varin, mon co-directeur de recherche. En plus de m'avoir donné l'opportunité de réaliser ce projet et d'avoir cru en mes compétences, leurs disponibilités, conseils, rigueur jusqu'aux moindres détails et soutiens quels que soient leur nature ont été d'une importance précieuse et m'ont permis de sortir bien outillé pour affronter les futurs défis professionnels.

Mes remerciements s'adressent également à tous les chercheurs, professionnels de recherche et personnel administratif du CERFO qui ont contribué pour que ce projet soit réalisé dans les meilleures conditions.

Je tiens également à remercier les professeurs Kalifa Goïta et Saeid Homayouni pour avoir accepté d'évaluer le mémoire.

Grande reconnaissance au Gouvernement du BURUNDI pour tout le soutien financier qu'il a pu mettre à ma disposition durant toutes mes années d'études universitaires.

J'aimerais finalement adresser mes remerciements à toute ma famille pour leur soutien inconditionnel et indéfectible tout au long de mon parcours, plus particulièrement à ma mère, à qui je dédie ce travail. A toi Maman, source inépuisable d'amour, de tendresse, tu m'as permis de voir ce soleil qui illumine mes journées, tu as guidé mes premiers pas et tu ne cesses jamais de prier pour moi, que Dieu t'accorde encore beaucoup de courage. Cette maîtrise, elle est pour toi.

1. Introduction

1.1. Mise en contexte

A travers le monde, la biodiversité est soumise à plusieurs sources de perturbation dont les activités humaines et la variation des conditions environnementales telles que celles associées aux changements climatiques (Kumar Rai et Singh, 2020). Le changement de ces conditions peut entrainer, dans des milieux naturels, la disparition d'espèces indigènes au profit de nouvelles espèces exotiques qui n'étaient pas présentes avant la perturbation. L'installation de ces nouvelles espèces est en partie possible suite au transport intentionnel ou non lors des mouvements de la population (Young et Larson, 2011). Le transport, l'installation et la prolifération de ces espèces dans ces nouveaux milieux peuvent engendrer des conséquences négatives (Kumar Rai et Singh, 2020). Elles deviennent ainsi des espèces exotiques envahissantes (EEE) dès lors que les impacts négatifs commencent à se manifester (Shine, 2007).

Les EEE végétales (EEEv) sont actuellement considérées comme étant l'une des causes principales de la perte de la biodiversité à travers le monde (Langmaier et Lapin, 2020; Paz-Kagan *et al.*, 2019; Guido et Pillar, 2017; Early *et al.*, 2016; IUCN Council, 2000). Des impacts d'ordre socio-économique sont également observés dans des milieux nouvellement envahis et varient selon la biologie de l'espèce et la vulnérabilité du milieu concerné (Jensen *et al.*, 2020; Roy *et al.*, 2019; Shackleton *et al.*, 2018). Ces impacts concernent, par exemple, les coûts liés à la gestion et l'éradication des EEEv, la perte de la valeur des terres envahies ainsi que les maladies provoquées par certaines de ces espèces (p. ex. dermatite au contact de la sève de certaines plantes telle que la berce du Caucase (*Heracleum mantegazzianum*)) (Kelsch *et al.*, 2020; Lavoie *et al*., 2014 ;Vilà *et al*., 2010).

1.2. Problématique

Face à cette menace, des méthodes efficaces et efficientes sont nécessaires afin de prévenir ces différents types d'impacts. Au Canada, la stratégie nationale sur les EEEv se concentre sur quatre axes principaux, à savoir la prévention de nouvelles invasions, la détection précoce de nouveaux envahisseurs, l'intervention rapide en présence de nouveaux envahisseurs ainsi que la gestion des EEEv qui sont établies ou qui se répandent (Environnement Canada, 2004). La réussite de cette stratégie nécessite des informations

relativement complètes et facilement interprétables en ce qui concerne la distribution territoriale et le niveau d'infestation par ces espèces. Ces données sur la répartition territoriale ont été, dans le passé, principalement acquises à partir des inventaires *in situ* relevés par positionnement GNSS (*Global Navigation Satellite Systems*) ou encore par interprétation des photos aériennes (Royimani *et al.*, 2019; Lawrence *et al.*, 2006). Cependant, ces méthodes nécessitent beaucoup de temps, et ne sont pas financièrement et techniquement adaptées, surtout lorsqu'il s'agit de grandes étendues ou lorsque les conditions topographiques ne sont pas favorables (Royimani *et al.*, 2019; Lawrence *et al.*, 2006). L'utilisation de la télédétection pourrait donc être une alternative plus favorable au suivi et gestion des EEEv (Dash *et al.*, 2019; Niphadkar, 2016). Cette technologie permet d'établir une distribution spatiale sur de vastes étendues et avec des intervalles de temps plus courts que les inventaires *in situ*, facilitant ainsi la détection précoce qui constitue un des facteurs de succès dans l'éradication, avant que des vastes étendues ne soient affectées (Dash *et al.*, 2019; Early *et al.*, 2016; Ustin *et al.*, 2002).

Plusieurs études utilisant des méthodes de classification automatique ou semi/automatique à partir des données de télédétection ont été réalisées (Rizaludin Mahmud *et al.*, 2020; Ewald *et al.*, 2020; Labonté *et al.*, 2020; Martínez-Sánchez *et al.*, 2019; Kattenborn *et al.*, 2019). Ces études ont démontré un potentiel intéressant de l'utilisation de la télédétection dans la gestion de ces invasions ainsi que la nécessité de développer des méthodes adaptées à chaque espèce et son environnement. Cependant, peu d'études se sont intéressées à la cartographie de plusieurs EEEv sur un même territoire et la plupart d'entre elles ont été réalisées dans des milieux naturels relativement homogènes et de faibles étendues (Michez *et al*., 2016; Ustin *et al.*, 2002). Certains milieux plus hétérogènes tels que les milieux urbains sont souvent envahis par plusieurs EEEv, ce qui pose des défis de gestion.

Au Québec, plusieurs EEEv occupent certains milieux terrestres et aquatiques (Lavoie *et al.*, 2014). La cartographie de la répartition complète de ces espèces n'a pas encore été réalisée, et les gestionnaires ne disposent que d'informations partielles collectées sur le terrain par positionnement GNSS, ou à travers la plateforme SENTINELLE mise en place par le Ministère de l'Environnement et de la Lutte contre les changements climatiques (MELCC, 2020), et qui permet de colliger des observations effectuées par le grand public. De plus, le potentiel de la télédétection pour l'aide à la détection précoce et la gestion des

EEEv sur notre territoire d'intérêt (agglomération de Québec) n'a pas encore été exploré. L'agglomération de Québec a en effet exprimé le besoin d'obtenir une cartographie complète de son territoire pour plusieurs EEEv, donnée qui servira notamment pour la planification de l'aménagement du territoire. Ce projet a été réalisé en collaboration avec le Centre d'enseignement et de recherche en foresterie (CERFO).

2. Objectif de recherche

L'objectif principal de cette étude consiste à réaliser une classification multi-espèce de cinq EEEv terrestres présentes dans l'agglomération urbaine de Québec. Il s'agit de la renouée du Japon (*Fallopia japonica*), du phragmite (*Phragmites australis*), de la berce du Caucase (*Heracleum mantegazzianum*), du nerprun bourdaine (*Frangula alnus*) et du nerpun cathartique (*Rhamnus cathartica*). Pour ce faire, les objectifs spécifiques suivants sont visés :

- Explorer l'utilisation des techniques d'apprentissage automatique et l'analyse orientée-objet;
- Explorer l'exploitation de l'imagerie multi-date à très haute résolution spatiale;
- Procurer une approche cartographique aux gestionnaires afin d'effectuer un suivi de la distribution spatiale de ces espèces et ainsi d'agir efficacement et rapidement vis-à-vis des risques sur les milieux.

3. Cadre théorique

3.1. Espèces exotiques envahissantes : définitions

Afin d'aider les gestionnaires à mieux appréhender la notion d'EEEv, la communauté scientifique ainsi que d'autres institutions environnementales ont proposé certaines définitions permettant de mieux comprendre dans quelle catégorie classer une espèce et agir correctement vis-à-vis de cette espèce. Ainsi, certaines études se sont intéressées à la clarification des termes utilisés pour qualifier les espèces nouvellement introduites dans un milieu (Gbedomon *et al.*, 2020; Colautti et MacIsaac, 2004; Richardson *et al.*, 2000). Avant de définir une EEEv, il est d'abord utile de définir une espèce exotique. L'Union internationale pour la conservation de la nature (IUCN) définit une espèce exotique comme toute espèce non indigène présente dans une autre aire géographique autre que celle de sa

répartition naturelle (IUCN Council, 2000). La même définition est également reprise par d'autres auteurs ou organisations (Gbedomon *et al.*, 2020 ; Lavoie *et al.*, 2014; Environnement Canada, 2004; Richardson *et al.*, 2000). Cependant, la qualification d'une espèce exotique comme envahissante est toujours une source de confusion. Cette confusion consiste principalement à savoir à quel moment une espèce exotique devient envahissante. Certains auteurs et organisations considèrent qu'une espèce devient envahissante au moment où l'espèce devient une source d'impacts négatifs sur le plan environnemental et socio-économique (Shine, 2007; Environnement Canada, 2004; IUCN Council, 2000), contrairement à d'autres qui proposent que le terme « envahissante » soit attribué à une espèce sans aucune considération liée à son impact dans son nouvel environnement (Gbedomon *et al.*, 2020; Lavoie *et al.*, 2014; Richardson *et al.*, 2000). Il serait donc plus préférable de qualifier une EEE végétale d'envahissante en tenant compte de la superficie déjà envahie par l'EEEv après son introduction (Richardson *et al.*, 2000). Richardson *et al.* (2000) indiquent qu'une espèce végétale serait qualifiée d'envahissante lorsque l'espèce s'est propagée sur une distance supérieure à 100 m pendant 50 ans pour les espèces se reproduisant par graine, et sur une distance supérieure à 6 m pendant 3 ans pour les espèces se reproduisant par rhizomes. En considérant les impacts observés de ces EEEv, les termes « nuisibles » ou « mauvaises herbes » seraient donc utilisés (Lavoie *et al.*, 2014; Richardson *et al.*, 2000). Il y a lieu de constater que si on tient compte de ces critères (superficie et impacts), une espèce exotique pourra être qualifiée de nuisible dans une région quelconque et non nuisible ailleurs. Ainsi, il serait important d'élaborer pour chaque région ou pays, une liste d'espèces ayant un impact négatif potentiel sur les écosystèmes. Au Québec, Lavoie *et al.* (2014) ont élaboré une liste d'EEEv nuisibles en tenant compte de leurs impacts sur les milieux.

3.2. Impacts d'espèces exotiques envahissantes

Les impacts d'EEEv sont nombreux et se répercutent sur plusieurs aspects d'ordre environnemental, économique et socio-sanitaire (Kumar Rai et Singh, 2020; Hussner *et al.*, 2017; Vilà *et al.*, 2011).

3.2.1. Impacts environnementaux

Selon Kumar Rai et Singh (2020), la réduction de la diversité spécifique des plantes indigènes, la modification des propriétés physico-chimiques des sols ainsi que la modification des régimes des feux de la zone concernée constituent les trois principaux types de mécanismes à travers lesquels les EEEv affectent les milieux envahis. En effet, les EEEv sont le plus souvent plus compétitrices par rapport aux espèces indigènes vis-à-vis des ressources (Boettcher *et al.*, 2021; Kalkman et *al.*, 2019; Martínez-Izquierdo *et al.*, 2016). Cela provoque par la suite une réduction/extinction de la végétation indigène, réduction de la productivité primaire, altération des processus physico-chimiques et de tout le fonctionnement des écosystèmes (Davies et Johnson, 2011). A titre d'exemple, le remplacement des espèces indigènes peut altérer la qualité et la stabilité des sols et ainsi accentuer les phénomènes d'inondations et d'érosion (Lavoie *et al.*, 2014 ; Kumar Rai et Singh, 2020). La renouée du japon, classée parmi les 100 pires espèces envahissantes au monde (Lavoie *et al.*, 2014), est l'une des EEEv qui forme des populations homogènes après la disparition d'espèces indigènes. Cette espèce accentue l'érosion des berges après son installation suite à la détérioration du système racinaire initialement présent (Colleran *et al.*, 2020; Lavoie *et al.*, 2014). Quant au régime de feu, l'un des exemples est celui des espèces d'*Acacia* pour lesquelles Shackleton *et al.* (2018) ont constaté qu'elles accentuaient l'intensité du feu suite à la modification du type de biomasse.

3.2.2. Impacts socio-économiques

Des pertes économiques directes et indirectes sont engendrées par la présence d'EEEv sur un territoire donné. D'après l'Agence canadienne d'inspection des aliments (ACIA) (2008), l'impact économique des EEEv est généralement lié aux coûts directs engagés lors des activités de contrôle et d'éradication (coûts des produits chimiques par exemple), aux pertes de la production agricole et forestière. A cela s'ajoutent d'autres coûts indirects et difficilement quantifiables liés à la dégradation des services écologiques. Les enjeux sociaux concernent les maladies provoquées par certaines EEEv, qui peuvent, par exemple, provoquer des brûlures mortelles au contact avec la peau (p. ex. la berce du Caucase), une perte de la valeur des biens immobiliers ou encore la réduction de l'attractivité des milieux naturels (ACIA, 2008).

3.3. Stratégies de lutte contre les espèces exotiques envahissantes végétales

La stratégie de lutte contre les EEEv constitue un ensemble d'actions permettant de protéger les écosystèmes contre les envahisseurs externes et susceptibles d'affecter négativement leur fonctionnement. La prévention et le contrôle sont les principales stratégies qui sont globalement reconnus comme piliers de lutte contre les EEEv (IUCN Council, 2000). Au Canada, la stratégie nationale sur les EEEv mise en place en 2004 se concentre sur quatre axes principaux à savoir la prévention de nouvelles invasions, la détection précoce de nouveaux envahisseurs, l'intervention rapide en présence de nouveaux envahisseurs ainsi que la gestion (éradication, confinement et contrôle) des EEEv qui sont établies ou qui se répandent (Environnement Canada, 2004). L'objectif principal de cette stratégie consiste à réduire le risque que représentent les espèces envahissantes sur les écosystèmes naturels et aquatiques, suite à leur introduction intentionnelle ou accidentelle (Agence canadienne d'inspection des aliments, 2008).

3.3.1. Prévention

La prévention concerne le contrôle de l'introduction de nouvelles espèces, mais aussi un suivi régulier des espèces déjà introduites qui sont susceptibles de devenir problématiques (Richardson et Thuiller, 2007). Elle constitue un outil essentiel et permet de réduire les coûts relatifs à leur éradication ou à la réparation des dommages causés après leur installation (Richardson et Thuiller, 2007; McNeely, 2001).

3.3.2. Détection précoce et intervention rapide

La détection précoce et l'intervention rapide sont intimement liées dans la mesure où l'intervention ne peut pas être réalisée sans que l'espèce n'ait été détectée et identifiée. La détection précoce devient donc une étape de grande importance lorsque l'espèce s'est déjà installée sur un territoire (Dash *et al.*, 2019; IUCN, 2000). Il s'avère donc indispensable de mettre en place des méthodes rapides de détection (Environnement Canada, 2004). Au Québec, l'une des mesures mises en place pour aider à une détection rapide d'EEEv est la plateforme SENTINELLE (MELCC, 2020) qui vise à permettre à la population de signaler la présence de toute espèce considérée comme exotique envahissante.

3.3.3. Gestion

La gestion rassemble l'éradication, le confinement et le contrôle. Cette stratégie s'applique, pour une espèce donnée, lorsque les mesures de prévention, de détection précoce et d'intervention rapide n'ont pu éviter l'installation de l'espèce (IUCN, 2000). L'éradication consiste à éliminer l'espèce du territoire, de manière mécanique, chimique et/ou biologique (Hussner *et al.*, 2017). Le confinement consiste à maintenir l'espèce dans une zone bien précise tandis que le contrôle désigne le suivi et la réduction des densités ou abondances de l'espèce dans les zones affectées (Environnement Canada, 2004; IUCN, 2000).

3.4. Identification et cartographie d'espèces exotiques envahissantes végétales à partir des relevés *in situ*

Dans cette approche, la cartographie d'EEEv nécessite la collecte des données liées à la distribution de l'espèce sur le territoire concerné. Ces données sur la répartition peuvent être acquises à partir d'inventaires terrain (Royimani *et al.*, 2019; Lawrence *et al.*, 2006). Selon Rew et Cousens (2001), les méthodes de cartographie par inventaire sont généralement l'échantillonnage complet et continu sur toute la zone selon une grille bien définie, l'échantillonnage discret qui se fait avec comptage d'individus à l'intérieur des quadrats préalablement choisis et les relevés par GNSS de tout individu présent sur la zone. Cependant, certaines de ces méthodes ne sont pas exhaustives et sont exigeantes en temps et en coûts (Somerville *et al.*, 2020).

3.5. Télédétection d'espèces exotiques envahissantes végétales

L'utilisation de la télédétection pour aider les gestionnaires à prévenir, détecter et contrôler les EEEv date de plusieurs années. Selon l'étude réalisée par Vaz *et al.* (2018), les premiers travaux datent de 1970, mais se sont véritablement développés à partir des années 2000. En plus de la disponibilité grandissante des données, c'est à partir de cette période que plusieurs programmes de gestion d'EEEv ont été mis en place, suscitant l'intérêt des chercheurs et gestionnaires au développement des méthodes de cartographie d'EEEv par télédétection (Vaz *et al.*, 2018). L'une des anciennes techniques utilisées dans la cartographie d'EEEv est la photo-interprétation (Royimani *et al*., 2019). Dans cette approche, un expert en photo-interprétation analyse les photos et cartographie la répartition de l'EEEv sur la scène. Par exemple, Müllerová *et al.* (2005) ont utilisé les photos aériennes

pour analyser la dynamique de l'invasion par la berce du Caucase (*Heracleum mantegazzianum*) sur une période de 50 ans. La tâche principale consistait à identifier et délimiter manuellement les régions envahies. C'est une approche qui a démontré un certain succès, mais le travail manuel nécessaire est très laborieux. Ces dernières décennies, d'autres méthodes de classification semi/automatiques et rapides ont été développées et permettent de contourner les principales limites de la photo-interprétation. Ces méthodes de classification utilisent différents types d'attributs (caractéristiques discriminantes) permettant une meilleure séparabilité entre les EEEv et les espèces indigènes. A ce jour, de nombreuses études ont donc été réalisées dans divers écosystèmes avec des approches diversifiées qui exploitant diverses caractéristiques discriminantes telles que la différence des propriétés spectrales entre les EEEv et les espèces indigènes (Ewald *et al.*, 2020; Niphadkar, 2016; Dorigo *et al.*, 2012; Sánchez-Azofeifa *et al.*, 2009; Asner *et al.*, 2008), la phénologie (Labonté *et al.*, 2020; Müllerová *et al.*, 2017; Dorigo *et al.*, 2012) et la morphologie (Kattenborn *et al.*, 2019; Franklin *et al.*, 2000). Différentes méthodes de classification semi/automatique telles que la forêt d'arbres aléatoires (*Random Forest-RF*) (Shiferaw *et al.*, 2019; Dash *et al.*, 2019; Martin *et al.*, 2018; Dorigo *et al*., 2012), les machines à vecteurs de support (*Support Vector Machines* - SVM) (Abeysinghe *et al*., 2019; Paz-Kagan *et al.*, 2019; Kganyago *et al.*, 2018) et les réseaux de neurones artificiels (Qian *et al.*, 2020; Abeysinghe *et al*., 2019) sont principalement utilisées.

3.5.1. Caractéristiques de discrimination utilisées

Dans ces études, différentes propriétés liées à l'absorption du rayonnement électromagnétique dans des domaines spectraux spécifiques tels que le visible, proche infra-rouge ou infra-rouge moyen, à la phénologie et à la morphologie sont principalement exploitées. L'utilisation des propriétés spectrales repose sur l'hypothèse de l'existence des différences en pigments photosynthétiques comme la chlorophylle (Sánchez-Azofeifa *et al*., 2009), permettant d'observer une séparabilité notable par l'utilisation d'indices spectraux. La phénologie est une autre propriété utilisée car plusieurs EEEv présentent un décalage de certains stades phénologiques avec les espèces indigènes (p. ex. floraison). C'est le cas de certaines EEEv décidues comme le nerprun bourdaine dont les feuilles apparaissent plus rapidement au printemps et disparaissent plus tard à l'automne (Becker *et al*., 2013; Xu *et al*., 2007). L'autre propriété est la morphologie mesurable par

l'utilisation d'indices de texture et de forme des objets dans une image (Kattenborn *et al*., 2019; Haralick, 1979). Le tableau 1 résume les différents types de caractéristiques de discrimination les plus exploitées ainsi que les types de données de télédétection principalement utilisés.

Tableau 1 : Critères et types de données utilisés pour la discrimination d'espèces exotiques envahissantes végétales

	Caractéristiques discriminantes utilisées	Indicateurs utilisés	Données utilisées	Contraintes	Référence
Phénologie	Stades phénologiques des espèces exotiques envahissantes (p. ex. floraison, senescence)	Réflectance et Indices de végétation (NDVI, *Excess green index*, *Leaf area index*….)	Images mono/multi-date à très haute résolution temporelle, spatiale et spectrale	Moins de capteurs à haute résolution temporelle avec très haute résolution spatiale	Yu, 2020; Müllerová *et al.*, 2017; Bradley, 2014; Ishii et Washitani, 2013; dorigo *et al.,* 2012; Wilfong *et al.*, 2009; Casady *et al*., 2005
Morphologie	Différences dans l'arrangement spatial des feuilles et branches	Indices de texture (p. ex. variance, entropie, …)	Images multispectrales à très haute résolution spatiale	Choix des indices et stratégie de calcul	Kattenborn *et al.*, 2019; Franklin *et al.*, 2000; Haralick, 1979
Biochimie des feuilles	Différences dans les constituants photosynthétiques et la structure des feuilles (p. ex. teneur en chlorophylle)	Réflectance dans les longueurs d'onde du visible et de l'infra- rouge (proche et moyen) et indices spectraux (NDVI, NDWI,…)	Images hyperspectrales à très haute résolution spatiale, seules ou en combinaison avec LiDAR	Traitements complexes	Ewald *et al.*, 2020; Rizaludin Mahmud *et al.*, 2020; Niphadkar, 2016; Sánchez-Azofeifa *et al.*, 2009; Asner *et al.*, 2008; Schnitzer, 2005

NDVI: *Normalized Difference Vegetation Index*, NDWI : *Normalized Difference Water Index*, LiDAR: *Light Detection and Ranging*

3.5.2. Méthodes de classification d'espèces exotiques envahissantes végétales

Plusieurs méthodes de classification d'images ont été utilisées pour cartographier les EEEv de manière semi/automatique (Royimani *et al*., 2019; Lu et Weng, 2007; Lass *et al*., 2005). Une revue globale réalisée par Lu et Weng (2007) décrit les différentes catégories des méthodes de classification d'images de télédétection. En télédétection d'EEEv, les méthodes adoptées sont essentiellement formées par les méthodes orientées-objet et les méthodes d'apprentissage automatique non paramétriques (Royimani *et al.*, 2019; Asner *et al.*, 2008; Lass *et al.*, 2005).

La classification orientée-objet consiste à grouper d'abord les pixels remplissant certains critères de similarité entre eux pour former des objets (groupes homogènes de pixels voisins) qui seront considérés comme unité de base de classification afin de leur assigner une classe d'intérêt (Chen *et al.*, 2014). Elle a l'avantage d'utiliser plusieurs types d'attributs spectraux et spatiaux (p. ex. attributs géométriques, de texture et topographiques) dans le processus de classification (Hantson *et al.*, 2012). Les unités de traitement étant des objets, elle permet de s'affranchir des problèmes fréquemment observés dans la classification orientée-pixel dont le phénomène de « poivre et sel » (Hirayama *et al.*, 2019; Chen *et al.*, 2014; Jones *et al.*, 2011).

Les méthodes d'apprentissage automatique non paramétriques sont des méthodes qui ne nécessitent pas que les données des échantillons d'entrainement soient normalement distribuées. Ces méthodes sont donc capables d'intégrer plusieurs types de données sans considération des paramètres statistiques de distribution des données d'entrainement. Dans ce sens, ces méthodes sont plus aptes à la classification des données multi sources souvent caractérisées par des distributions statistiques distinctes (Benediktsson et Sveinsson, 1997). Elles sont également intéressantes lorsque le nombre d'échantillons pour certaines classes est faible surtout dans les milieux plus hétérogènes (p. ex. zones urbaines) où il peut être difficile de trouver suffisamment d'échantillons pour certaines classes (Masse, 2013). Les méthodes utilisées dans plusieurs travaux de classification d'EEEv sont la forêt d'arbres aléatoires (*Random Forest-RF*), les machines à vecteurs de support (*Support Vector Machines* - SVM) et les réseaux de neurones artificiels (Qian *et al.*, 2020; Shiferaw *et al.*, 2019, Paz-Kagan *et al.*, 2019; Dash *et al.*, 2019; Kganyago *et al.*, 2018; Dorigo *et al.*, 2012). Le *Random Forest* est constitué d'un ensemble d'arbres de décision qui affectent

individuellement un objet/pixel à une classe et le résultat final est obtenu par un vote majoritaire sur l'ensemble des résultats produits par chacun des arbres de décision (Breiman, 2001). Pour SVM, il s'agit d'une méthode basée sur l'utilisation des hyperplans ou surfaces de décision qui maximisent la distance marginale entre les échantillons des classes (deux ou plusieurs classes) à séparer, appelés vecteurs de support (Noble, 2006). Quant aux réseaux de neurones artificiels, il s'agit des méthodes qui ont suscité un intérêt particulier en télédétection ces dernières années (Zhang *et al.*, 2016). Ces sont des méthodes d'apprentissage formées par des couches d'entrée (images initiales à classer) et de sortie (classes d'intérêt) reliées par un algorithme d'apprentissage qui fonctionne par rétro-propagation afin de minimiser l'erreur d'identification (Lee, 2018). Ces méthodes nécessitent des processus d'optimisation par essais-erreur ou par validation croisée longs. Elles nécessitent également plusieurs variables d'entrée, des outils de traitement performants et un délai d'entrainement et de classification très long (Qian *et al*., 2020; Royimani *et al*., 2019; Lantz et Wang, 2013; Kavzoglu et Mather, 2004). Cependant, plusieurs études ont mis en évidence leurs performances. Martin *et al.* (2018) ont notamment obtenu une précision globale supérieure à 90 % en utilisant RF pour cartographier la renouée du Japon (*Fallopia japonica*) dans la zone d'Anse et Serrière (France). Des résultats d'une précision globale de 95 % ont également été obtenus par Dorigo *et al*. (2012) qui ont utilisé RF pour cartographier la renouée du Japon à Ljubljana (Slovénie). Les réseaux de neurones et SVM ont été utilisés par Abeysinghe *et al.* (2019) pour la détection du phragmite (*Phragmites australis*) en Ohio (États-Unis) et ont obtenu une précision globale respective de 94 % et 90 %. Des méthodes récemment développées telles que *Extreme Gradient Boosting* (XGBoost) (Zarei *et al*., 2021; Sagi et Rokach, 2021; Samat *et al*., 2020) auraient également un potentiel intéressant pour la cartographie d'EEEv. La méthode XGBoost consiste en un ensemble d'arbres décisionnels dits faibles (*weak learners*) (Zarei *et al*., 2021) ajoutés de manière séquentielle afin de réduire la valeur de la fonction de perte (*loss function*) et ainsi réduire l'erreur de prédiction. Cette méthode a été utilisée et comparée à RF dans une étude de cartographie d'une EEEv *Opuntia stricta* au Kenya réalisée par James *et al.* (2021). Les résultats obtenus avec une bonne précision (précision globale de 89 % avec XGBoost et 92,4 % pour RF) montrent l'intérêt d'explorer

l'application de ces nouvelles méthodes d'apprentissage automatique pour cartographier les EEEv.

3.5.3. Sources de données

Il existe plusieurs sources de données disponibles pour la cartographie d'EEEv par télédétection (tableau 2). La revue de littérature montre que les images multispectrales de très haute à moyenne résolution spatiale sont les plus utilisées. La partie du spectre électromagnétique utilisée est principalement celle du visible et du proche infra-rouge. Par contre, les images hyperspectrales, données LiDAR et radar sont moins utilisées. L'absence de l'utilisation de ces données s'explique principalement par leur grande exigence en expertise, en moyens de traitement et en coûts d'acquisition (Royimani *et al.*, 2019; Vaz *et al.*, 2018).

Tableau 2 : Source de données utilisées en télédétection d'espèces exotiques envahissantes végétales

Source de données	Catégorie d'images	Domaine spectral utilisé	Références
Landsat	Multispectrale	Visible et PIR	Yu, 2020; Labonté *et al*., 2020; Becker *et al*., 2013; Wilfong *et al*., 2009
Sentinel-1	Radar (VV et VH)	Bande C	Kattenborn *et al*., 2019
Sentinel-2	Multispectrale	Visible et PIR	Kattenborn *et al*., 2019
SPOT-7	Multispectrale	Visible et PIR	Abutaleb *et al*., 2020
Ikonos	Multispectrale	Visible et PIR	Lawrence *et al*., 2006; Casady *et al*., 2005
WoldView-2	Multispectrale	Visible et PIR	Rizaludin Mahmud *et al*., 2020; Abutaleb *et al*., 2020; Paz-Kagan *et al*., 2019; Fernandes *et al*., 2014; Lantz et Wang, 2013
WoldView-3	Multispectrale	Visible-PIR- IROC	Shendryk *et al*., 2020
Capteurs aériens	Hyperspectrale et LiDAR	Visible-PIR-IROC	Ewald *et al*., 2020 Kattenborn *et al*., 2019; Marvin *et al*., 2016; Ishii et Washitani, 2013; Asner *et al*., 2008
Capteurs aériens drones (UAV)	Multispectrale	Visible et PIR	Qian *et al*., 2020; Kattenborn *et al*., 2019; Müllerová *et al*., 2017 Fernandes *et al*., 2014; Dorigo *et al*., 2012
Capteurs terrestres	Hyperspectrale	Visible-PIR- IROC	Rizaludin Mahmud *et al*., 2020

UAV: *Unmanned Aerial Vehicle*, SPOT-7 : Satellite Pour l'Observation de la Terre-7, PIR : Proche Infra-rouge, IROC : Infra-rouge ondes courtes, VV : Polarisation Verticale-Verticale, VH : Polarisation Vertical-Horizontale, LiDAR*: Light Detection and Ranging*

4. Cartographie d'espèces exotiques envahissantes végétales à l'aide d'images satellites à très haute résolution spatiale multi-date, en utilisant des techniques d'analyse orientée-objet et d'apprentissage automatique: une étude comparative

L'article scientifique présentant les résultats de cette étude a été soumis au journal scientifique *GIScience & Remote Sensing*, le 04 Août 2022 (preuve de soumission : annexe 1). Afin de faciliter la lecture, la numérotation des titres, figures, tableaux et annexes a été modifiée.

Mapping invasive alien plant species with very high spatial resolution and multi-date satellite imagery using object-based and machine learning techniques: A comparative study

Nininahazwe Fiston[a,b,c,*], Jérôme Théau[a,c], Marc-Antoine Genest[b], Mathieu Varin[b]
[a]*Département de Géomatique appliquée, Université de Sherbrooke, 2500 boul.Universté, QC J1K2R1, Sherbrooke, Canada*
[b]*Centre d'enseignement et de recherche en foresterie (CERFO), 2440 Ch.Ste-Foy, QC G1V 1T2, Québec, Canada*
[c]*Centre de la science de la biodiversité du Québec, 1205 Av. du Docteur-Penfield S3/18, QC H3A 1B1, Montréal, Canada*

**Corresponding author Email : Fiston.nininahazwe@usherbrooke.ca*

Abstract :

Invasive alien plant species (IAPS) have negative impacts on ecosystems, including the loss of biodiversity and the alteration of ecosystem functions. The strategy for mitigating these impacts requires knowledge of these species' spatial distribution and level of infestation. *In situ* inventories or aerial photo interpretation can be used to collect these data but they are labour-intensive, time-consuming, and incomplete, especially when dealing with large or inaccessible areas. Remote sensing may be an effective method of mapping IAPS for a better management strategy. Several studies using remote sensing to map IAPS have focused on single species detection and were conducted in relatively homogeneous natural environments, while other common, more heterogeneous environments, such as urban areas, are often invaded by multiple IAPS, posing management challenges. The main objective of this study was to develop a mapping method for three major IAPS observed in the urban agglomeration of Québec city (Canada), namely Japanese knotweed (*Fallopia japonica*), giant hogweed (*Heracleum mantegazzianum*) and phragmites (*Phragmites australis*)). Mono-date and multi-date classification approaches were used with

WorldView-3 and SPOT-7 satellite imagery, acquired in the summer of 2020 and in the autumn of 2019, respectively. To estimate presence probability, object-based image analysis (OBIA) and nonparametric classifiers such as Support Vector Machines (SVM), Random Forest (RF) and Extreme Gradient Boosting (XGBoost) were used. Overall, multi-date classification using WorldView-3 and SPOT-7 images produced the best results, with a Kappa coefficient of 0.85 and an overall accuracy of 91% using RF. Individual class performances based on F1-score revealed that Japanese knotweed had the highest maximum value (0.95), followed by giant hogweed (0.91) and phragmites (0.87). These results confirmed the potential of remote sensing to accurately map and simultaneously monitor the main IAPS in a heterogeneous urban environment using a multi-date approach. Although the approach is limited by image and reference data availability, it provides new tools to managers for IAPS invasion control.

Keywords: Invasive alien species, remote sensing, multi-date, satellite imagery, OBIA, machine learning

4.1. Introduction

Invasive alien plant species (IAPS) are currently considered to be one of the main causes of biodiversity loss worldwide (Langmaier and Lapin, 2020; Paz-Kagan *et al*., 2019; Guido and Pillar, 2017; Early *et al*., 2016; IUCN Council, 2000). In addition to this environmental impact, management and eradication costs, loss of invaded land value, and health problems caused by certain IAPS are also important impacts (Kelsch *et al*., 2020; Roy *et al*., 2019; Shackleton *et al*., 2018; Lavoie *et al*., 2014).

The strategy designed to limit these impacts consists of the prevention of new invasions, the detection of early stage invasions rapid response, and management of established or spreading IAPS (IUCN Council 2000). The success of this strategy requires the most accurate information possible regarding the spatial distribution and levels of infestation of IAPS.

In the past, datasets of the territorial distribution of IAPS were mainly acquired from *in situ* inventories collected by GNSS (Global Navigation Satellite Systems) or via the interpretation of aerial photos (Royimani *et al*., 2019; Lawrence *et al*., 2006; Müllerová *et al*., 2005). However, these methods are labour-intensive and often not financially and technically suitable, especially when dealing with large or inaccessible areas. They can also be relatively subjective because they are observer-dependent (Royimani *et al*., 2019; Lawrence *et al*., 2006). The use of remote sensing

may be a more favourable alternative for monitoring and managing IAPS (Dash *et al*., 2019; Niphadkar, 2016). Easily replicable approaches allow to map spatial distribution over large areas in much shorter time than *in situ* inventories, allowing early detection, which is one of the success factors of IAPS eradication before large areas are invaded (Dash *et al*., 2019; Early *et al*., 2016; Ustin *et al*., 2002).

Automatic classification methods have been developed in recent decades to overcome the main limitations of field inventory-based methods (Royimani *et al*., 2019; Lu and Weng, 2007; Lass *et al*., 2005). In particular, object-based image analysis (OBIA) and nonparametric (e.g., machine learning techniques) approaches (Royimani *et al*., 2019; Asner *et al*., 2008; Lass *et al*., 2005) have been widely used.

OBIA consists of first grouping adjacent pixels, fulfilling certain criteria of similarity between them to form objects (i.e., homogeneous groups of neighbouring pixels) which will be considered as the basic unit of classification, and to then assign them a class of interest (Chen *et al*., 2014). OBIA has the advantage of using several types of spectral and spatial features (e.g., geometry, texture, topography) in the classification process (Hantson *et al*., 2012). Since the processing units are objects, the approach avoids the problems frequently observed in pixel-based classification approaches, such as salt-and-pepper noise (Hirayama *et al*., 2019; Chen *et al*., 2014; Jones *et al*., 2011).

Nonparametric machine learning techniques do not require a normal distribution of training samples and are therefore able to combine multiple data sources often characterized by distinct statistical distributions (Benediktsson and Sveinsson, 1997). These methods are also suitable for small samples, especially in heterogeneous environments (e.g., urban areas) where it may be difficult to find enough samples for certain classes (Masse, 2013).

Random Forest (RF), support vector machines (SVM) and artificial neural networks (Qian *et al*., 2020; Shiferaw *et al*., 2019, Paz-Kagan *et al*., 2019; Dash *et al*., 2019; Kganyago *et al*., 2018; Dorigo *et al*., 2012) are the most used machine learning techniques for IAPS classification. Although these techniques require powerful tools related to optimization, training and classification as well as a high number of input feature requirements (Qian *et al*., 2020; Royimani *et al*., 2019; Lantz and Wang, 2013; Kavzoglu and Mather, 2004), several studies have highlighted their strong performance. As an example, Martin *et al*. (2018) achieved an overall accuracy of more than 90% using RF to map Japanese knotweed (*Fallopia japonica*) in the Anse and Serrières area (France).

An overall accuracy of 95% was also obtained by Dorigo *et al*. (2012) using RF to map Japanese knotweed in Ljubljana, Slovenia. Artificial neural networks and SVM classification were used by Abeysinghe *et al*. (2019) for the detection of phragmites (*Phragmites australis*) in Ohio, USA, achieving 94% and 90% overall accuracy, respectively.

These machine learning techniques also have the potential to incorporate different types of arithmetic discriminative features to distinguish IAPS from native species. Their spectral properties in the visible, near-infrared or mid-infrared range, their phenology and morphology are the attributes mainly used (Ewald *et al*., 2020; Niphadkar, 2016; Dorigo *et al*., 2012). Most IAPS have high concentrations of photosynthetic pigments (Sánchez-Azofeifa *et al*., 2009; Asner *et al*., 2008; Castro-Esau *et al*., 2004), allowing significant separability from native species. Castro-Esau *et al*. (2004) found a decrease of classification error from 16 to 4% for two invasive and other native species following the addition of chlorophyll content. Phenology is also used, because some of the vegetative stages (e.g., flowering) of certain IAPS occur at different times than native species. This characteristic can be exploited by remote sensing using bi-temporal images or indices and has been successfully used (overall accuracy = 95%) to map Japanese knotweed using aerial images acquired in winter and summer in Ljubljana (Slovenia) (Dorigo *et al*., 2012). Morphology is measurable using texture and shape indices of objects in an image (Kattenborn *et al*., 2019; Haralick, 1979), and allows the discrimination of IAPS from native species when characterized by a particular shape or coloration (Müllerová *et al*., 2017; Michez *et al*., 2016; Jones *et al*., 2011). Texture indices were exploited in a mapping study of giant hogweed (*Heracleum mantegazzianum*) (overall accuracy = 97%) and relevant discriminant texture indices appeared to be related to the white coloration of umbels, which allowed the extraction of discriminating homogeneity indices (Michez *et al*., 2016).

Relatively few studies have focused on mapping multiple IAPS in the same area, and most have been carried out in relatively homogeneous natural environments over small areas (Michez *et al*., 2016; Ustin *et al*., 2002). Heterogeneous environments such as urban areas are often invaded by multiple IAPS, leading to management challenges. Curiously, the few studies that have focused on this type of environment have focused on a single IAPS and have not exploited discriminating characteristics such as phenology (Kazmi *et al*., 2021; Martin *et al*., 2018; Singh *et al*., 2018).

The main objective of this study was to exploit the use of machine learning techniques and OBIA applied to multi-date images to perform a multi-species classification of IAPS in a complex urban area.

4.2. Materials and methods

4.2.1. Study area

The study area is the urban agglomeration of Québec city (Québec, Canada) and covers a total surface area of 557 km^2 (Figure 1). The natural environment consists of forest, urban woodlands, wetlands and water bodies (City of Québec, 2006). The forest, which occupies mainly the northern and western zones, represents about 35% of the total area, of which 44% is deciduous and 42% is mixed (deciduous and coniferous). Several areas of the urban agglomeration of Québec city are invaded by IAPS (Lavoie *et al*., 2014).

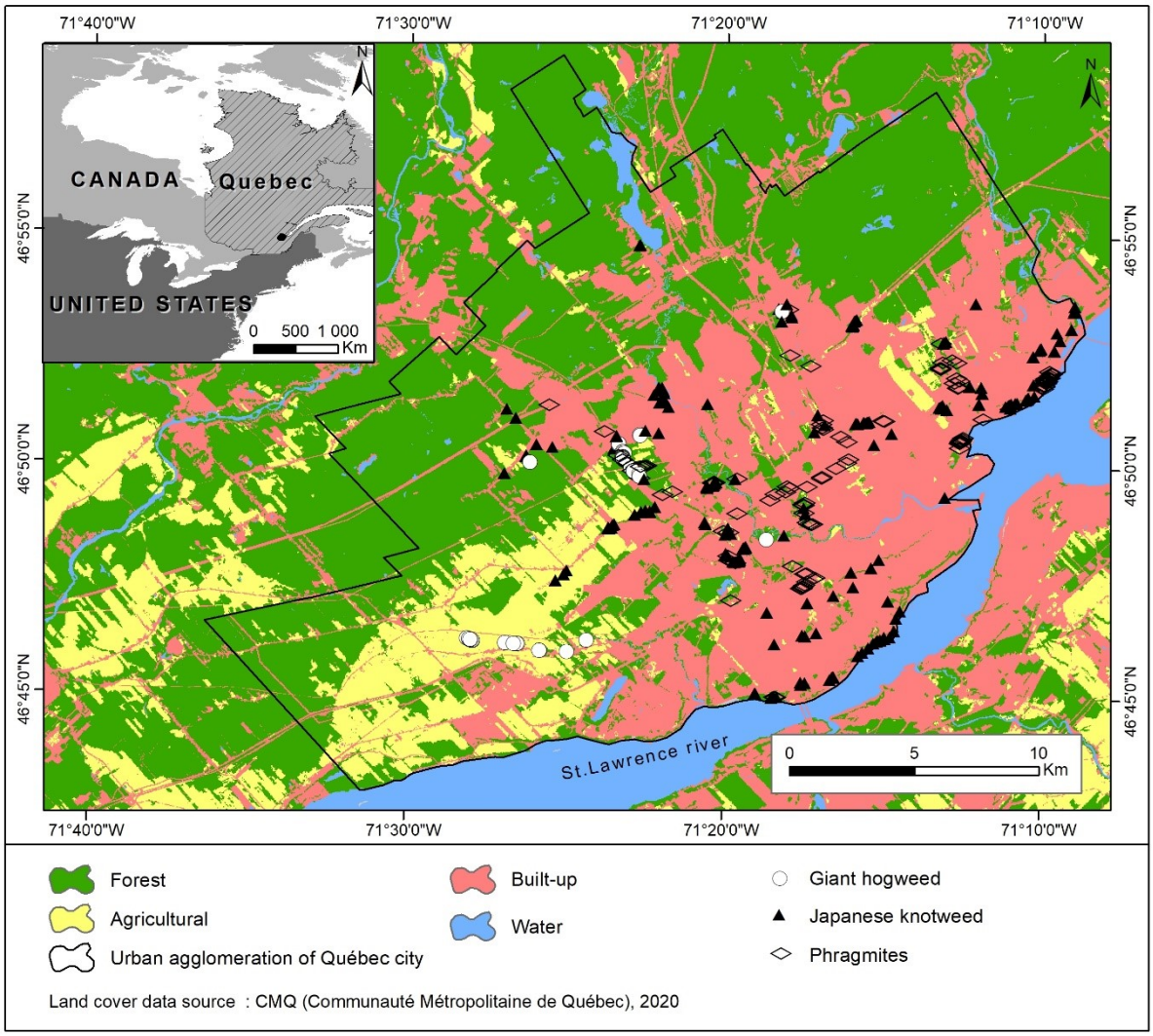

Figure 1 : Study area limits and reference data locations of invasive alien plant species (giant hogweed, Japanese knotweed and phragmites).

4.2.2. Studied species

The species considered in this study are terrestrial IAPS, namely Japanese knotweed, phragmites and giant hogweed. Originally from East Asia and introduced to North America as an ornamental species, Japanese knotweed is considered one of the world's top 100 worst invasive species (Lavoie *et al*., 2014; Dorigo *et al*., 2012). The species forms dense and homogeneous colonies mainly along roads, railways, riparian areas and other urban environments and can grow up to 3 m tall (Aguilera *et al*., 2010) (Figure 2a). This species causes the loss of biodiversity as a result of its proliferation and the modification of the hydrographic network as a result of the resistance that its root system imposes to runoff (Dorigo *et al*., 2012; Collingham *et al*., 2000). Its highly developed root system represents one-third of its biomass and explains the very high eradication costs, which requires large-scale excavation (Lavoie *et al*., 2014).

Giant hogweed is a species native to the Caucasus region of Central Asia (Page *et al*., 2006). It can exceed a height of 3 m and mainly colonizes stream edges, agricultural ditches and forest edges (Page *et al*., 2006) (Figure 2c). This species has a negative impact on biodiversity, accelerates water erosion and cause human health threats due to inflammatory toxic secretions (Lavoie *et al*., 2014; Page *et al*., 2006).

Phragmites is originally from Eurasia and develops dense colonies over 2 m tall primarily in marshes, road and agricultural drainage ditches (Abeysinghe *et al*., 2019; Lavoie *et al*., 2014) (Figure 2e). Stems can sometimes damage road construction, reduce the presence of native species and alter habitat for aquatic species such as fish (Abeysinghe *et al*., 2019; Lavoie *et al*., 2014; Leonard *et al*., 2002).

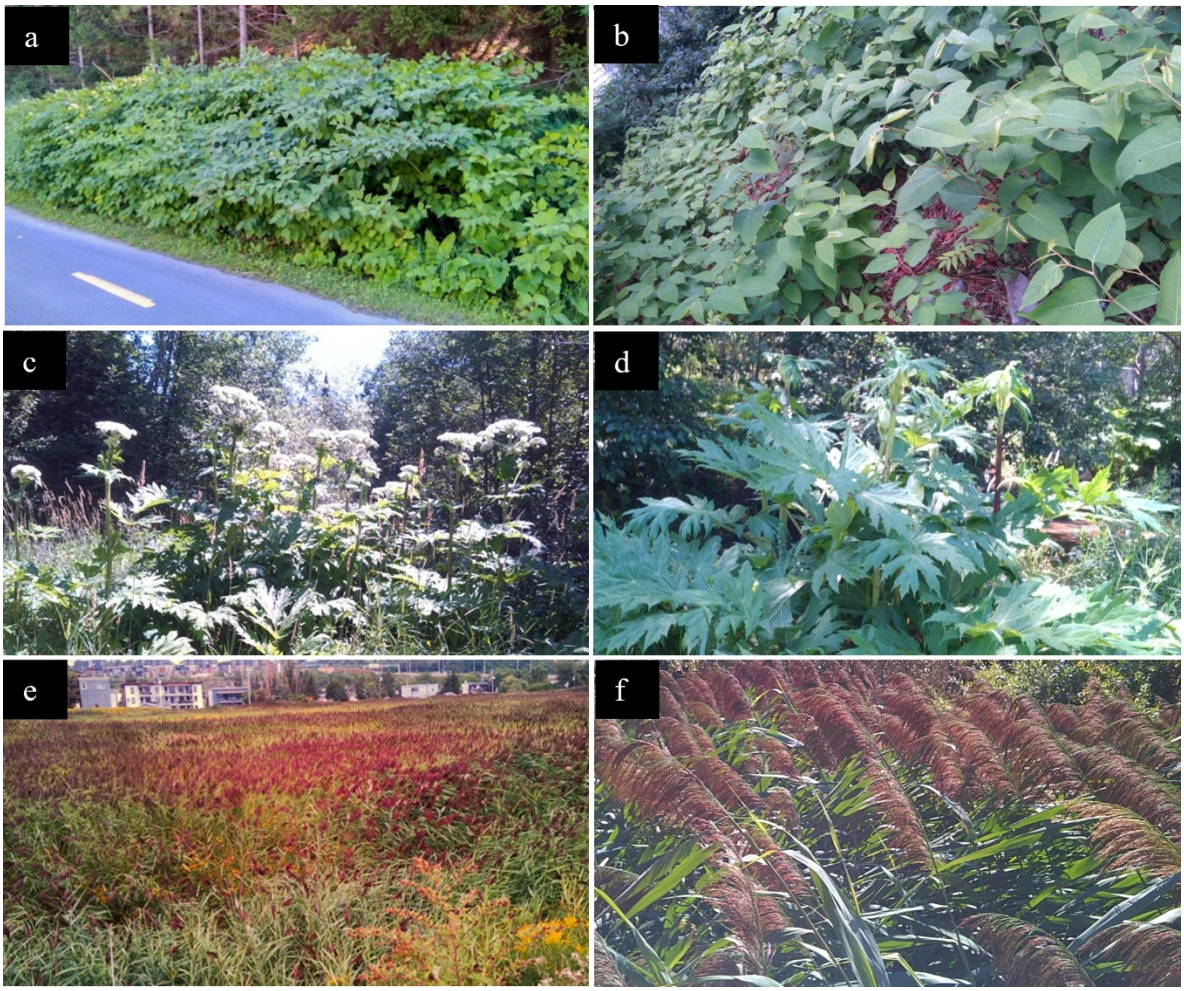

Figure 2 : Field photography of invasive alien plant species at two zoom levels. Japanese knotweed (a, b), giant hogweed (c, d), phragmites (e, f).

4.2.3. Field reference data collection

Field campaigns were conducted between June 26 and August 26, 2020. Previously known invaded sites were systematically visited and each new site identified in the field was also characterized. Points and polygons of IAPS and absences were collected using Xplore Bobcat (Xplore Technologies, Texas) and Blackview (Blackview, Shenzhen) electronic tablets connected to GNSS receivers (Pro 6 H GNSS (Trimble, California) and Arrow Gold (EOS positioning system, Quebec)). Polygons were digitized *in situ* based on a RGB orthomosaic (red-green-blue, 15 cm spatial resolution, acquired in summer 2018) aerial imagery. Giant hogweed point data collected in 2019 by managers of the Cap Rouge River watershed council were also added to the database after validation of their presence in 2020 using photo-interpretation. A total of 283, 128, 76 and 32

points and polygons were used for absences, Japanese knotweed, phragmites and giant hogweed, respectively.

4.2.4. Image acquisition

This study used multi-source satellite imagery, namely WV-3/WV110 satellite images (WorldView-3/World View 110 camera) and SPOT-7/NAOMI (Satellite Pour l'Observation de la Terre - 7/ New AstroSat Optical Modular Instrument) acquired in summer and autumn, respectively, in order to explore the contribution of these phases to the classification. The characteristics of the images are presented in Table 3.

Table 3 : Characteristics of satellite images used in this study

Image	Band	Wavelength range (center) (nm)	Spatial resolution (m)	Acquisition date
WV-3	Coastal	400 – 450 (425)	1.24	2020/07/06
	Blue	450 – 510 (480)		
	Green	510 – 580 (545)		
	Yellow	585 – 625 (605)		
	Red	630 – 690 (660)		
	Red Edge	705 – 745 (725)		
	Near-infrared #1	770 – 895 (832.5)		
	Near-infrared #2	860 – 1040 (950)		
	Panchromatic	450 – 800 (625)	0.31	
SPOT-7	Blue	450 – 520 (485)	6	2019/10/26
	Green	530 – 590 (560)		
	Red	625 – 695 (660)		
	Near-infrared	760 – 890 (825)		
	Panchromatic	450 – 745 (597.5)	1.5	

WV-3 : WorldView-3, SPOT-7 : Satellite Pour l'Observation de la Terre-7

4.2.5. Image pre-processing and classification

Two main steps were performed for IAPS mapping: (1) pre-processing, including atmospheric correction (this step was performed to normalize multi-source images digital value to the same reflectance range between 0 and 1), fusion of panchromatic and multispectral bands, orthorectification and masking to remove irrelevant areas; and (2) classification of the segmented objects by machine learning techniques. The flowchart of the study is presented in Figure 3.

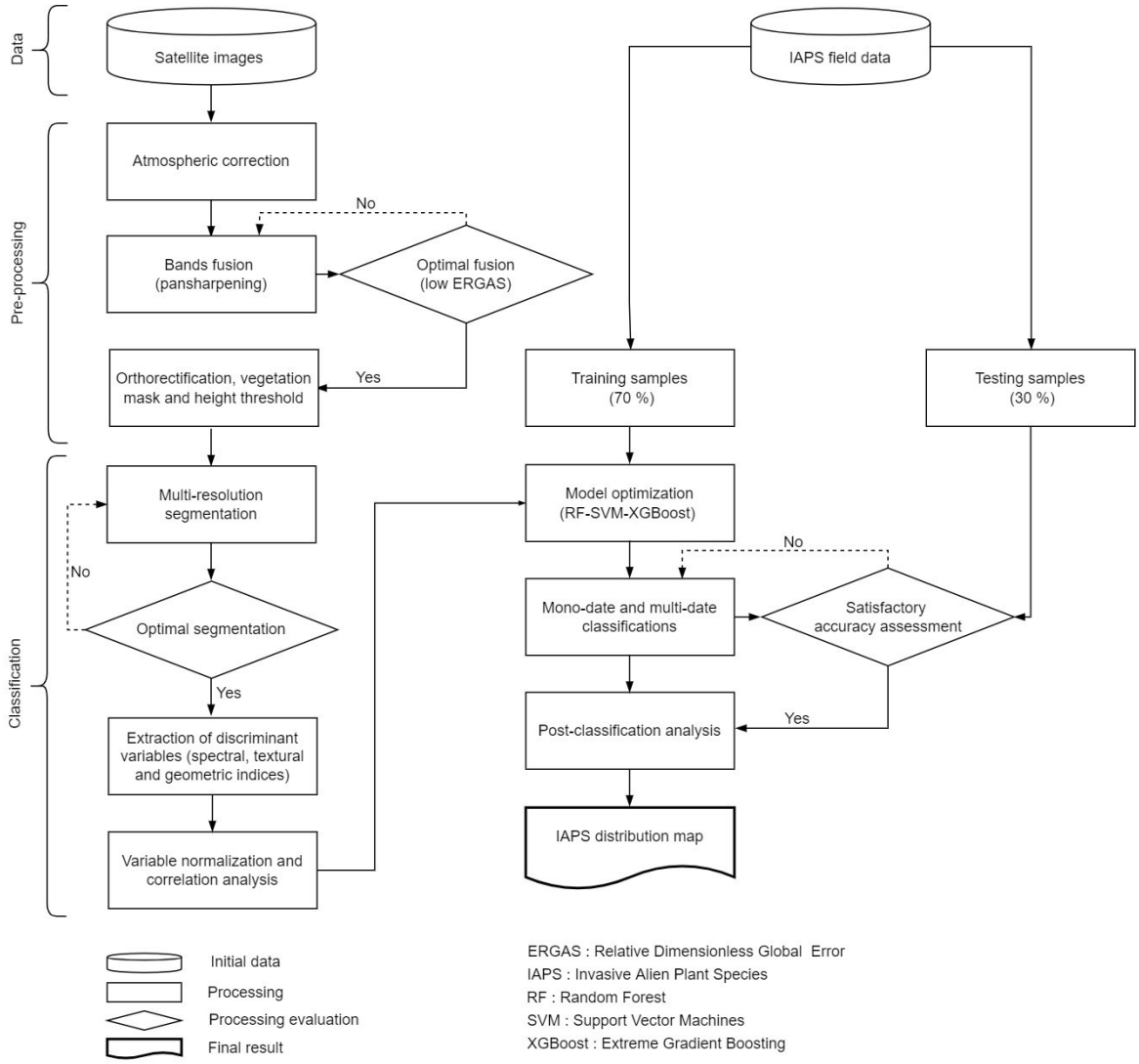

Figure 3 : Methodological flowchart of the study

4.2.5.1. Image pre-processing

Atmospheric corrections were performed using the ATCOR module (PCI Geomatics, 2018). Spatial resolution enhancement (i.e., pansharpening) of the multispectral bands by fusion with the panchromatic band was also applied. The Zhang (Zhang, 2004), Gram-Schmidt (GS) (Belfiore *et al*., 2016), ratio component substitution (RCS), local mean and variance matching (LMVM) and Bayesian fusion (Grizonnet *et al*., 2017) methods were compared. The method that minimizes the relative dimensionless global error (ERGAS) index was selected. This index is calculated from the root mean square of error (RMSE) according to equations (1) and (2) and evaluates the distortion of the spectral information in the pansharpened images (Park *et al*., 2020; Li *et al*., 2017; Belfiore *et al*., 2016; Ranchin *et al*., 2003); values close to zero are more relevant to minimizing of spectral information of pansharpened images (Mhangara *et al*., 2020, Li *et al*., 2017; Ranchin *et al*., 2003).

$$\mathrm{RMSE} = \sqrt{\frac{1}{m \times n} \sum_{i=1}^{m} \sum_{j=1}^{n} [\mathrm{M(i,j)} - \mathrm{F(i,j)}]^2} \quad (1)$$

$$\mathrm{ERGAS} = \frac{100}{\mathrm{R}} \sqrt{\frac{1}{\mathrm{N}} \sum_{\mathrm{k}=1}^{\mathrm{N}} \frac{\mathrm{RMSE_k}^2}{\mathrm{M_K}^2}} \quad (2)$$

Where M (i, j) is the spectral value of the original band pixel at position (i, j), F (i, j) is the spectral value of the pansharpened band pixel at position (i, j), R is the resolution ratio between the multispectral bands and the panchromatic band, N is the number of bands, k is the band number, and M_k is the mean of the original band k.

To optimize the processing time, four of the fourteen WV-3 tiles representative of the different environments and occupying half of the study area were selected for this analysis. Spectral bands whose wavelength does not correspond to that of the panchromatic band (i.e., Coastal and Near-infrared #2) were not used for this analysis and were resampled to 0.31 m using the bilinear interpolation method. The fusion methods were each compared to the WV-3 images and the optimal method thereby identified was used for the SPOT-7 image fusion. The LMVM and RCS methods showed the best results compared to the other methods (Table 4).

Table 4 : ERGAS (Relative Dimensionless Global Error) values for the fusion methods applied to the WorldView-3 image

	Zhang	Bayesian fusion	RCS	LMVM	GS
Tile 1	2.80	2.31	2.03	2.03	2.87
Tile 2	4.24	3.72	3.40	3.08	4.31
Tile 3	6.17	7.43	4.80	4.34	5.40
Tile 4	3.98	3.13	2.95	2.59	3.53
Mean ± SD	4.30 ± 0.94	4.15 ± 1.64	3.30 ± 0.81	3.01 ± 0.70	4.03 ± 0.83

RCS: Ratio Component Substitution, LMVM: Local Mean and Variance Matching,
GS: Gram-Schmidt, SD: Standard Deviation

While the LMVM method performed slightly better according to the ERGAS, the RCS method was selected because it presents a better compromise between minimizing spectral distortion and improving the geometric structure of the objects (see Appendix 3).

The pansharpened images were orthorectified using a digital terrain model (Varin *et al*., 2020) and a second-order polynomial function was performed before tile mosaicking using the Bundle colour balancing method (PCI Geomatics, 2018). Control points were identified from an orthomosaic of aerial images acquired in summer 2018 at 15 cm spatial resolution. The images were orthorectified with a RMSE of 0.63 pixels for WV-3 and 0.50 pixels for SPOT-7, and the respective spatial resolutions after fusion were 0.31 m and 1.5 m.

4.2.5.2. Masking

Three masks were applied to exclude areas not suitable for the selected IAPS. A normalized difference vegetation index (NDVI) threshold (NDVI < 0.37) was used to eliminate non-vegetated areas (i.e., bare soil, buildings, and water bodies) using the minimum average of reference objects corresponding to the four classes. A second mask, based on a digital height model (Varin *et al*., 2020), was applied to exclude vegetation higher than 4 m. This threshold is based on field observations and the literature (Abeysinghe *et al*., 2019; Lavoie *et al*., 2014; Barney *et al*., 2006). Finally, a shadow index (SI) was used (Zhou *et al*., 2018) to eliminate shaded areas (SI ≤ 13.13). This threshold was selected based on a sample of 60 objects representing shadows on the WV-3 orthomosaic (i.e., the maximum average identified for all 60 objects).

4.2.5.3. Multi-resolution segmentation

WV-3 orthomosaic segmentation was used for object generation because it was acquired at higher spatial resolution than the SPOT-7 image. To eliminate redundancy of spectral bands (Bilgin *et al*., 2011; Kermad and Chehdi, 2000) and to optimize processing time, the Red-edge, Near-infrared#1, green and red bands were selected for segmentation after analysis of spectral separability using the Jeffries-Matusita distance (JM) between classes (Oktorini *et al*., 2021; Massetti *et al*., 2016).

The Estimation of Scale Parameter method (ESP2) (Drăguţ *et al*., 2014; Drăguţ *et al*., 2010) was used as a tool to assist in identifying the optimal scale. Twelve tiles of equal size (20000 × 20000 pixels) in which IAPS were identified were selected to analyse the local variance at each object level (Drăguţ *et al*., 2010). Different combinations of scale, colour, and shape (compactness) were tested until the optimal values of 25 for scale, 0.9 for colour and 0.5 for shape were reached, as well as a weight equal to 1 for each of the four bands used.

4.2.5.4. Extraction and pre-processing of discriminant features

Three categories of arithmetic features, as well as spectral, textural and geometric ones were calculated using eCognition Developer 10.1 software (Trimble Geospatial, USA). The categories and formulas for the features computed for each of the images (152 for WV-3, 78 for SPOT-7) are presented in Table 3. The features were centred and scaled over all the study area dataset, and a correlation analysis was performed to eliminate redundant ones. If two features were correlated with a Pearson coefficient greater than or equal to 0.85 (Varin *et al.,* 2020), the feature that achieves better separability according to the JM separability distance was used.

Table 5 : Extracted features (spectral, textural and geometric) for classification modeling

Category	Feature	Definition	Reference
Spectral	Mean	All	
	Maximum	All	
	Standard deviation	All	
	95^{th} percentile	All	
	Skewness	All	
	NDVI (Normalized Difference Vegetation Index)	(NIR#1 - red) / (NIR#1 + Red)	Carlson et Ripley (1997)
	RENDVI (Red-Edge Normalized Difference Vegetation Index)	(NIR#1 - RE) / (NIR#1 + RE)	Waser *et al.* (2014)
	VARI (Visible Atmospherically Resistant Index)	(green - red) / (green + red -blue)	Gitelson *et al.* (2002)
	RGR (Red Green Ratio)	red / green	Zhou *et al.* (2021)
	SR (Simple Ratio)	NIR#1 / red	Zhou *et al.* (2021)
	BTBR (Bi-Temporal Band Ratio)	(red, green)*	Dorigo *et al.* (2012)
	HSI (Hue, Saturation, Intensity)	red, green, blue*	Chaudhary *et al.* (2012)
	CI (Colour index)	(red - green) / (red + green)	Escadafal *et al.* (1991)
	BI (Brightness index)	$(red^2 + NIR\#1\ ^2)^{0.5}$	Zhou *et al.* (2018)
	NDWI (Normalized Difference Water Index)	(green - NIR#1) / (green + NIR#1)	Zhou *et al.* (2018)
	NIR-RE ratio	(NIR#1 - 3.06 × RE) / (1.71× NIR#1 - 2.42 × RE - 4.14)	Developped by the research team
Textural	GLCM (Gray Level Co-occurrence Matrix): contrast, correlation, entropy, homogeneity, Angular second moment, mean, standard-deviation) GLDV (Gray Level Difference Vector): contrast, entropy, mean, angular second moment	All	Haralick (1979)
Geometric	Width, length, compactness	-	

NIR : Near-infrared, RE : Red-Edge

*Because of limited space, only the bands used are indicated (see references for detailed definition).

4.2.5.5. Classification approach

Five classifications were compared, with two mono-date classifications using only features calculated from each of the two images (WV-3 and SPOT-7) performed first. Two additional classifications were then performed by adding the multi-date BTBR index developed by Dorigo *et al.* (2012) to each of these images (WV-3 + BTBR, SPOT-7 + BTBR). This index (equation (3)) consists of combining the spectral properties of two phenological periods. Finally, a classification combining features from both images including BTBR (WV-3 + SPOT-7 + BTBR) was performed.

$$\mathrm{BTBR} = \frac{\frac{R_{off}}{R_{on}} - \frac{G_{off}}{G_{on}}}{\frac{R_{off}}{R_{on}} + \frac{G_{off}}{G_{on}}} \quad (3)$$

Where R and G indicate the reflectance values in the red and green bands, respectively. The suffixes indicate the image acquisition periods (the growing season (on) and the senescence period (off)).

4.2.5.6. Machine learning techniques and optimization

Three machine learning techniques : RF (Breiman, 2001), SVM (Guenther and Schonlau, 2016) and XGBoost (Zarei *et al*., 2021; Samat *et al*., 2020) classifiers were tested and compared. The selection of important discriminant features for each classifier was performed using the recursive feature elimination (RFE) selection method with ten-fold cross-validations (Yang *et al*., 2019; Guyon *et al*., 2002; Ambroise and McLachlan, 2002). Subsequently, the caret package in R (R core team, 2021) was used to optimize the other parameters of the three classifiers. The value of mtry (i.e., the number of random features used at each node) for RF was the one that minimized the out of bag error (OOB), and the number of decision trees (ntree) was the one at which this minimal OOB error was considered constant. In the SVM, the radial basis function was used, and the cost and sigma parameters, as well as the XGBoost parameters, such as the learning rate, were automatically optimized by performing all possible combinations between 10 values of each parameter (i.e., a tune length of 10). A classifier that optimizes the user and producer accuracies (i.e., for high F1-score averages) was used for the prediction of object membership in classes. The class with the highest prediction probability was assigned to the object.

4.2.5.7. Accuracy assessment

The reference data were overlaid with the objects from the segmentations, and for each class, the corresponding segments were divided between training segments (70%) and validation segments (30%), chosen randomly. Cohen's Kappa coefficient (Congalton, 1991; Cohen, 1960) and overall accuracy were calculated for global accuracy assessment. User accuracy, producer accuracy and F1-score were also calculated for individual class performance analysis (Costa *et al*., 2021; Yang, 2001).

4.2.5.8. Post-classification analysis

Several criteria were used to exclude certain areas that were not suitable for the selected IAPS. Giant hogweed and phragmites do not colonize areas near residences (Lavoie *et al*., 2014; Page *et al*., 2006; Barney *et al*., 2006), and so prediction of these species was not performed within 10 m of residential buildings. Agricultural areas were also excluded, except parcel edges (10 m or less from edges) that may be invaded by these species.

4.3. Results

4.3.1. Mono-date classification

Classification using just the WV-3 orthomosaic showed that the XGBoost classifier performed better (Kappa = 0.81) than the RF (Kappa = 0.77) and SVM classifiers (Kappa = 0.74) (Table 6). The performances obtained using the WV-3 orthomosaic are much better than those obtained from the SPOT-7 image classification (Kappa = 0.48 (SVM), 0.44 (RF) and 0.41 (XGBoost)).

Classification performances for individual classes also showed that the WV-3 orthomosaic features discriminate classes better than SPOT-7, according to the F1-score. Japanese knotweed (maximum F1-score = 0.93, RF) and giant hogweed (maximum F1-score = 0.90, SVM) were better classified using the WV-3 orthomosaic than phragmites (maximum F1-score = 0.71, XGBoost) with the same orthomosaic. For all IAPS, the F1-score values were less satisfactory and did not exceed 0.65 regardless of classifier when the SPOT-7 image was used (Table 6).

Table 6 : Performance measures of classifiers. The values in bold correspond to the maximum performance values.

		WV-3			WV-3 + BTBR			SPOT-7			SPOT-7 + BTBR			WV-3 + SPOT-7 + BTBR		
		RF	SVM	XGBoost	RF	SVM	XGBoost	RF	SVM	XGBoost	RF	SVM	XGBoost	RF	SVM	XGBoost
	Kappa	0.77	0.75	0.81	**0.85**	0.80	0.81	0.44	0.48	0.41	0.64	0.65	0.49	**0.85**	0.80	0.81
	OA	0.87	0.85	0.89	**0.91**	0.88	0.89	0.70	0.72	0.66	0.80	0.80	0.70	**0.91**	0.88	0.89
Japanese knotweed	UA	0.90	0.87	0.90	0.88	0.83	0.90	0.67	0.74	0.47	0.77	0.81	0.58	0.88	0.85	0.85
	PA	0.97	0.94	0.97	0.97	0.97	1.00	0.50	0.47	0.58	0.67	0.72	0.64	0.97	0.92	0.94
	F1-score	0.93	0.91	0.93	0.92	0.90	0.95	0.57	0.58	0.52	0.72	0.76	0.61	0.92	0.88	0.89
Phragmites	UA	1.00	0.75	0.92	1.00	0.84	0.88	0.77	0.75	0.80	0.93	0.88	0.72	0.94	0.84	1.00
	PA	0.52	0.57	0.57	0.76	0.76	0.67	0.48	0.57	0.38	0.67	0.71	0.62	0.81	0.76	0.76
	F1-score	0.69	0.65	0.71	0.86	0.80	0.76	0.59	0.65	0.52	0.78	0.79	0.67	0.87	0.80	0.86
Giant hogweed	UA	0.78	0.82	0.90	0.82	0.82	0.80	1.00	0.75	0.33	0.80	0.60	0.50	0.82	0.83	0.80
	PA	0.70	0.90	0.90	0.90	0.90	0.80	0.20	0.30	0.20	0.40	0.30	0.20	0.90	1.00	0.80
	F1-score	0.74	0.86	0.90	0.86	0.86	0.80	0.33	0.43	0.25	0.53	0.40	0.29	0.86	0.91	0.80
Absence	UA	0.85	0.86	0.88	0.92	0.91	0.90	0.69	0.71	0.76	0.78	0.80	0.76	0.93	0.90	0.90
	PA	0.93	0.87	0.93	0.92	0.86	0.91	0.89	0.91	0.81	0.93	0.92	0.80	0.91	0.87	0.91
	F1-score	0.89	0.87	0.90	0.92	0.88	0.90	0.78	0.79	0.78	0.85	0.85	0.78	0.92	0.89	0.90
Mean (F1-score)		0.81	0.82	0.86	**0.89**	0.86	0.85	0.57	0.61	0.52	0.72	0.70	0.58	**0.89**	0.87	0.87
SD (F1-score)		0.10	0.09	0.08	0.03	0.03	0.07	0.12	0.11	0.13	0.09	0.15	0.15	0.03	0.03	0.03

OA: Overall Accuracy, PA: Producer Accuracy, UA: User Accuracy, SD: Standard Deviation, RF: Random Forest, SVM: Support Vector Machines, XGBoost: Extreme Gradient Boosting

4.3.2. Multi-date classification

4.3.2.1. Mono-date features combination with BTBR (WV-3-BTBR and SPOT-7-BTBR)

RF was the best performing classifier, with a Kappa coefficient of 0.85 when the BTBR index was added to theWV-3 orthomosaic (increasing the Kappa coefficient from 0.77) (Table 6). The Kappa coefficient value for SVM also increased, from 0.75 to 0.80, while this coefficient remained constant for XGBoost (0.81) when the BTBR was incorporated. The reduction in confusion between phragmites and absences after incorporation of the BTBR index (maximum F1-score = 0.86 versus 0.71 for WV-3) improved the performance indicators. The Kappa coefficients were also increased for the SPOT-7 image, from 0.44 to 0.64 for RF, 0.48 to 0.65 for SVM and 0.41 to 0.49 for XGBoost.

Individual classification performances between IAPS varied when comparing the addition of BTBR. For WV-3, there was an increase of the maximum F1-score value of 0.02 for Japanese knotweed and 0.15 for phragmites, whereas the maximum F1-score value was reduced by 0.04 for giant hogweed (Table 6). This suggests that the use of BTBR provides more benefits for phragmites than for the other two IAPS. The use of BTBR also improved the IAPS classification performance with SPOT-7 according to the F1-score. For RF, for example, the improvement is 0.15, 0.19, and 0.20 for Japanese knotweed, phragmites and giant hogweed, respectively. However, these values are still lower than those obtained for WV3 + BTBR and do not exceed 0.79 (Table 6).

4.3.2.2. Multi-date features combination with BTBR (WV-3 + SPOT-7 + BTBR)

The performance of the three classifiers after the features from both images were combined with BTBR is similar to that obtained for WV-3 + BTBR, and better than that obtained for SPOT-7 + BTBR. RF remains the optimal classifier for classification of all three IAPS, with Kappa = 0.85, Kappa = 0.81 for XGBoost and Kappa = 0.80 for SVM (Table 6). The only difference observed between WV-3 + BTBR and WV-3 + SPOT-7 + BTBR is the F1-score value, which increases very slightly from 0.86 to 0.87 for phragmites. The combination of WV-3 + SPOT-7 + BTBR and RF was therefore used for the prediction and mapping of the three IAPS in the study area.

4.3.3. Invasive alien plant species mapping

Some representative examples of IAPS mapping after membership prediction using the RF classifier (WV-3 + SPOT-7 + BTBR) are shown in Figure 4. The objects identified as phragmites are mainly located along highways, drainage ditches and around water bodies (Figure 4a and 4b).

Identified giant hogweed plants are usually located along streams and woodland edges and in clearings under the canopy (Figure 4a and 4c). Large concentrations of Japanese knotweed were generally observed along trails, railroads and vacant lots (Figure 4d). The particularity of this species is its presence along the fences of houses where it had often been installed for ornamental purposes (Figure 4d).

The total area of the three IAPS detected is 455 ha and represents 0.8% of the study area. The area of phragmites (378 ha) is much larger than that of Japanese knotweed (68 ha) and giant hogweed (9 ha). However, this area could be underestimated for phragmites and overestimated for Japanese knotweed and giant hogweed, based on the accuracy assessment measures (Table 6). The omission error (1-PA) for phragmites was 19%, while the commission error (1-UA) was 6% (RF, WV-3 + SPOT-7 + BTBR). The classifier was unable to predict some phragmites objects, but omitted more than it committed. A post-processing verification showed that objects classified as absence correspond to low densities of phragmites (Figure 5a) and areas where phragmites were not yet in the flowering stage (Figure 5b).

Omission errors (1-PA) for Japanese knotweed and giant hogweed were 3 and 10%, respectively, while errors of commission (1-UA) were 12% and 18%, respectively. There were more absence objects incorrectly classified as these IAPS than those in the phragmites class. The presence of several plant species, including species spectrally similar to Japanese knotweed and giant hogweed (e.g., staghorn sumac (*Rhus typhina*) and wild red raspberry (*Rubus idaeus*)) could be considered as sources of the errors observed for these two IAPS (Figure 6).

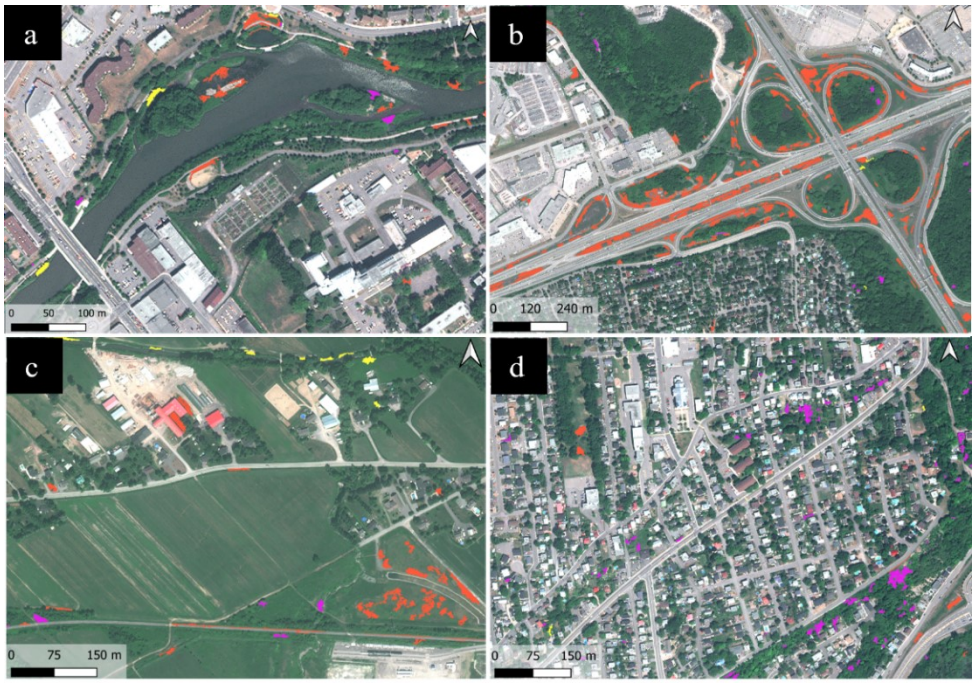

Figure 4 : Examples of invasive alien plant species detected in four types of environment : riverbanks (a), roadsides (b), agriculture ditches (c), and residential areas (d). Species are indicated in yellow (giant hogweed), orange (phragmites), and purple (Japanese knotweed).

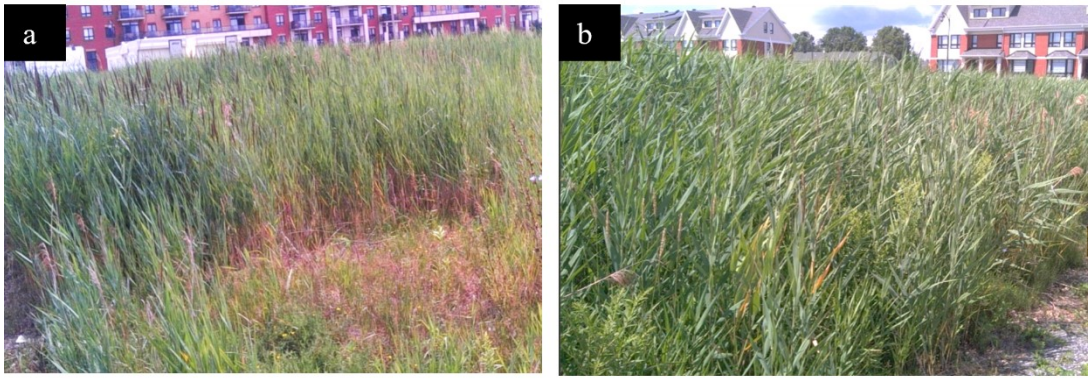

Figure 5 : Examples of phragmites stands not detected. Phragmites at low density (a) and a phragmites stand before flowering stage (b) (field photography from 30th July 2020).

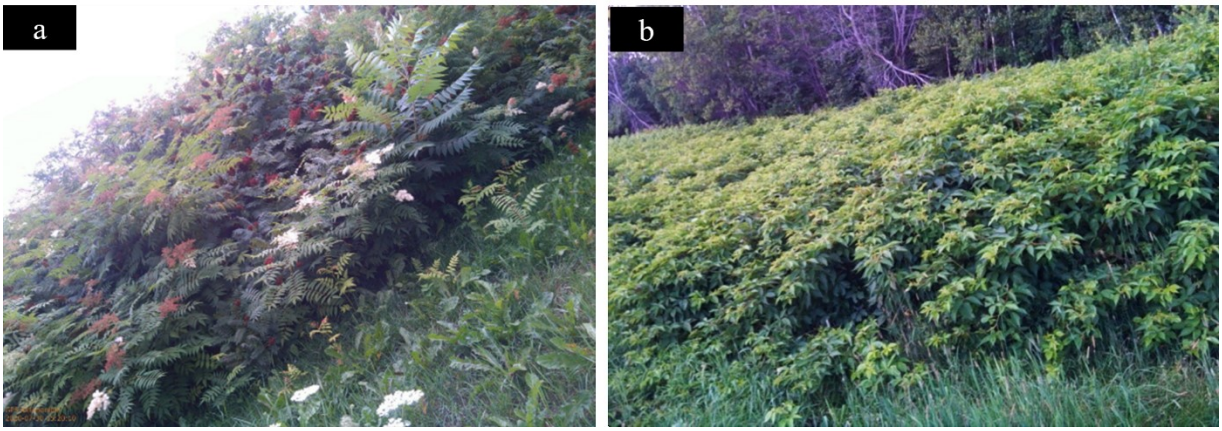

Figure 6 : Examples of non-invasive alien plant species classified as Japanese knotweed (commission errors). Field photography of staghorn sumac (*Rhus typhina*) from 30th July 2020 (a) and wild red raspberry (*Rubus idaeus*) from 29th July 2020 (b).

4.4. Discussion

4.4.1. Global performances of multi-species classification

4.4.1.1. Mono-date classification

According to the range of performances based on the Kappa coefficient (Monserud, 1990), very good performance was achieved with the mono-date classification (maximum Kappa coefficient = 0.81, XGBoost) for WV-3, while the classification with the SPOT-7 image was fair (maximum Kappa = 0.48, SVM).

Compared to the few studies that have mapped several IAPS over the same territory, the performances obtained for WV-3 (maximum overall accuracy = 91%) were comparable to that obtained by Ustin *et al*. (2002) (maximum overall accuracy > 90%) who mapped four IAPS (different from those in this study) in California (USA) from AVIRIS hyperspectral images acquired in summer.

However, our results showed better performances compared to those obtained by Michez *et al*. (2016) who mapped Japanese knotweed and purple jewelweed (*Impatiens glandulifera*) using aerial images acquired in autumn (50 cm spatial resolution) in a riparian area in southern Belgium (overall accuracy = 72%). The variability of luminosity in autumn (between acquisition campaigns), the presence of shadows as well as a low coverage of targeted species were identified as the main factors related to their errors of classification. However, they obtained better results compared to ours with the use of SPOT-7 images, also acquired in autumn. In our study, this fair

performance could be related to the acquisition period (autumn) and the low separability between classes at this time of year (senescence for all species studied). Another source of classification errors could be related to low spatial resolution (6 m before pansharpening) compared to WV-3 (1.24 m before pansharpening) and the images used by Michez *et al*. (2016) (50 cm). Spectral mixing would therefore be higher in the SPOT-7 image than in the WV-3 image and would reduce classification performance (Labonté *et al*., 2020; Michez *et al*., 2016).

4.4.1.2. Multi-date classification

The combination of multi-date features including the BTBR index resulted in excellent performances (maximum Kappa = 0.85), higher than those obtained for mono-date classification (maximum Kappa = 0.81). These results highlight the significant contribution of the BTBR, which has also been shown in other studies carried out in similar environments. As an example, Martin *et al*. (2018) obtained a 61% detection rate for Japanese knotweed mapping by adding the modified BTBR (MBTBR) to the bands of the Pléiades images used. This detection rate was 50% and 59% when mono-date bands from autumn and summer were used, respectively. Dorigo *et al.* (2012) also obtained very good performance with an overall accuracy of 93% for mapping Japanese knotweed using multi-date drone images combined with the BTBR.

In addition to the BTBR, the most relevant features are the transformations of the initial bands, mainly vegetation indices and features from the IHS (Intensity, Hue, Saturation) transformation. These features are mostly WV-3-derived and represent 70% of the features used by the best classifier (WV-3 + SPOT-7 + BTBR, RF). The under-representation of the features calculated from the SPOT-7 image once again confirms the low contribution of this image type.

The textural features and means of the spectral bands were the least-used features in the classifiers. Apart from the entropy of the red band of the SPOT-7 image, no other textural features are present among the 25 most important features identified by the RF method. However, some studies have demonstrated the importance of texture in the classification of IAPS such as Japanese knotweed and giant hogweed (Michez *et al*., 2016; Dorigo *et al*., 2012). In our study, this result is not surprising, although colonies of some species, such as Japanese knotweed, are easily visible in the images. The spatial resolution of the images, the size of the IAPS patches and the level of separability from other native species are the main factors that influence the effectiveness of these features (Dorigo *et al*., 2012). Given that the WV-3 orthomosaic is at very high resolution and would be adequate for the use of texture to discriminate IAPS, the low contribution of texture

features in this study could therefore be attributed to the presence of several native plant species with high intraspecific variability that are spectrally similar to the IAPS studied (e.g., staghorn sumac and wild red raspberry).

Among the means of the spectral bands, only the red-edge band was selected and ranked 1st out of the 25 relevant features (determined by the Gini index (Breiman, 2001)). In contrast, derived features such as maximum, skewness and standard deviation were selected (i.e., 11 out of 25). The absence of the mean features from the spectral bands in this study is in contradiction with the results obtained by other authors. Michez *et al*. (2016) noticed that the mean features from the RGB drone images were among the most important features in the classification of IAPS, including Japanese knotweed. This difference could be explained by the different composition of native species (i.e., many native species in our study area are similar to IAPS in the visible bands). It is therefore important to note that the use of this methodology in another environment should be adapted, taking into account each environment specificity, especially the composition of native plant species.

4.4.2. Individual class performances

4.4.2.1. IAPS spatial distribution

One of the major challenges in the classification of IAPS is to collect enough reference data to build robust and easily generalizable models. For the phragmites, for example, very dense patches are often located along highways, which limits access to these samples for modelling. Some of the reference data used are thus less representative (e.g., lower density), reducing the classification performances of this species due to spectral mixing. More specifically, a verification showed that several omission errors for this species were related to low density phragmites objects, which was also observed by Rupasinghe and Chow-Fraser (2021), who found that low cover negatively affected phragmites' classification performance. Giant hogweed reference data are also difficult to access because of the systematic control (removal) conducted annually in the study area.

This lack of reference data creates an imbalance between absence data and the other classes, affecting classification performances (Pranto and Paul, 2021; Richhariya and Tanveer, 2020; More and Rana, 2017). The ratio of absence to IAPS data is approximately 2, 4 and 10 for Japanese knotweed, phragmites and giant hogweed, respectively. One reason for the poor performances of SVM compared to RF and XGBoost could be related to this imbalance between classes. Several authors have found that some classifiers, such as SVM, are more sensitive to highly unbalanced data (Gašparović and Dobrinić, 2020; Richhariya and Tanveer, 2020; Lemnaru and Potolea, 2012;

Nguyen *et al*., 2011; Akbani *et al*., 2004) than classifiers based on decision trees such as RF and XGBoost (Gašparović and Dobrinić, 2020; Zhao *et al*., 2018; More and Rana, 2017).

In addition to the use of less sensitive learning classifiers, other alternative techniques that involve undersampling the majority class or oversampling the minority class by creating new synthetic samples (e.g., Synthetic Minority Oversampling Technique) can be used (Patil *et al*., 2020; Lin *et al*., 2018; Fernandez *et al*., 2018; More and Rana, 2017). However, these techniques should be used with caution, as undersampling can reduce the diversity of absence data, especially in diverse environments such as our study area (Patil *et al*., 2020; Xu *et al*., 2019). Oversampling can also create highly correlated and interdependent synthetic data, which could imply a reduction in the efficiency of certain methods for selecting relevant features (Blagus and Lusa, 2013). A collaborative data collection and the sharing platforms of IAPS distribution are alternatives to improve access to reference data (e.g., the SENTINELLE platform of the Quebec government's Ministry of Environment and Climate Change).

4.4.2.2. Acquisition date and very high spatial resolution satellite images availability

The high performance for Japanese knotweed and giant hogweed with the WV-3 orthomosaic alone seems to be related to the optimal acquisition period. The month of July corresponds to the period when Japanese knotweed patches are well developed and delimited, which can facilitate detection using an OBIA approach. Giant hogweed is also in flowering season and the white umbels visible in the WV-3 image helped to discriminate them from other species (Michez *et al*., 2016). This result is financially and technically interesting, as the use of multi-date images often requires additional financial costs and potentially energy-consuming image co-registration and calibration processing. This study therefore shows the effectiveness of using a single very high spatial resolution image (WV-3) for these two IAPS when acquired at the optimal period.

For phragmites, the poor performance compared to the other two IAPS can be related to a non-optimal acquisition period. The SPOT-7 image is less efficient for reasons mentioned in the previous sections, and the WV-3 image was acquired in July before its flowering (occurs in August). It is during the flowering period that the spectral signature of phragmites is most distinct from the rest of the surrounding vegetation (Rupasinghe and Chow-Fraser, 2021). For example, a study using WV-2/3 satellite imagery acquired during the optimal flowering period to detect phragmites resulted in an overall accuracy of 93% (Rupasinghe and Chow-Fraser, 2021). When a mono-date image acquired at the optimal period for this species is not available, multi-date images

can therefore be an interesting alternative to improve phragmites detection, as illustrated by the increase of the F1-score performance in our study (0.71 to 0.87). Other studies have also demonstrated that using multi-date images can improve classifier performance for this species (Rupasinghe and Chow-Fraser, 2019; Abeysinghe *et al*., 2019; Poulin *et al*., 2010). Abeysinghe *et al*. (2019) achieved 94% overall accuracy for phragmites detection using multi-date very-high spatial resolution drone images. Rupasinghe and Chow-Fraser (2019) also obtained good performances (overall accuracy = 88%) using medium spatial resolution (Landsat7/8 and Sentinel-2) imagery to map phragmites.

However, the availability of both very high spatial and spectral resolution images is an important limitation in a context where multi-date images are needed to simultaneously map several IAPS with different optimal phenological periods. On the other hand, medium spatial resolution imagery (e.g., Landsat and Sentinel-2), more easily accessible and available, can be used when the objective is to detect patches whose size is greater than or equal to that of the image pixel (Wang *et al*., 2022). For small IAPS patch detection, especially in the case of early detection, fusion techniques (e.g., super-resolution) between medium and high spatial resolution images can be useful (Chen *et al*., 2020).

Super-resolution is a technique of deriving high-resolution images from low spatial resolution images (Wang *et al*., 2022; Müller *et al*., 2020; Shermeyer and Van Etten, 2019). Some of the most widely used techniques are based on deep learning (Wang *et al*., 2022; Bachir *et al*., 2021). For example, PlanetScope (3 m) and Sentinel-2 (10 m) images, acquired every day and every five days, respectively, can easily be available at optimal times. New multispectral band images with better spatial resolution can therefore be created to improve the classification obtained from initial low/medium spatial resolution images. Shermeyer and Van (2019) were able to achieve a 36% improvement in the detection accuracy of several objects (e.g., cars, airplanes, and boats) using super-resolution to increase the resolution of WV-3 images (30 cm to 15 cm). However, this technique has been less-used for IAPS detection (Chen *et al*., 2020). A few studies have highlighted the potential of this technique to improve detection (Chen *et al*., 2020; Shermeyer and Van Etten, 2019; Pouliot *et al*., 2018). Although this technique is demanding in computational resources, expertise and processing time, it should be explored for IAPS classification from medium spatial resolution images when very high spatial resolution images are not available or accessible. In fact, this technique was tested in our study for phragmites detection using the fusion between Sentinel-

2 (10 m) and Planetscope (3 m) images acquired during the flowering period (August 2020), and between SPOT-7 and GeoEye-1 images acquired in autumn (November 2020, 0.5 m) with two different deep-learning based techniques, residual convolutional neural networks (Latte and Lejeune, 2020) and enlighten-generative adversarial networks (Gong *et al.,* 2021), respectively. The performances were poor compared to the other approaches previously presented (Kappa < 0.5). Again, we hypothesize that the low density of colonies could explain these low accuracies for Sentinel-2 and Planetscope images, while the non-optimal acquisition period could explain the low accuracies obtained with SPOT-7 and GeoEye-1 images. This approach could therefore be improved by using a higher amount of representative reference data and by improving the timing for the images. It would also be interesting to explore classifications based on class density to properly identify the potential of applying super-resolution with medium (often available during optimal period) and high spatial resolution images.

4.5. Conclusion

This study was conducted in an urban heterogeneous environment and produced a multi-species classification of three IAPS using a multi-date approach, with good performances. These results demonstrate the potential of remote sensing to monitor IAPS in such an environment with high spatial satellite images. For operational purposes, the mapped areas of presence can be used for the monitoring and control of these IAPS that colonize several types of environments in the study area. The main limitations of this methodology are linked to the small amount of reference IAPS data, the high cost of very high spatial resolution and multi-date images, and the low availability of these images at optimal phenological periods of detection. Further studies are therefore needed to analyse the mapping performance of IAPS in similar environments using easily available images (e.g., Sentinel-2 and Landsat acquired during optimal periods) combined with techniques such as super-resolution.

4.6. Disclosure statement

No potential conflict of interest was reported by the author(s).

4.7. Acknowledgments

The authors gratefully acknowledge Nicolas Turcotte-Major (Québec city), Camille Armellin (CERFO), Anne-Marie Dubois (CERFO), Jean Marchal (CERFO), Julie Deslandes (Québec city), Mustapha Ramdani (Québec city), Andréanne Hains (Cap Rouge River watershed council) and Nicolas Latte (University of Liège) for their support during the project.

4.8. Funding

This study was supported by the Mitacs Accélération program, award number IT16759 and by the city of Québec.

4.9. Data availability statement

The data that support the findings of this study are openly available in the Open Science Framework data repository.

4.10. References

Abeysinghe T., Simic Milas A., Arend K., Hohman B., Reil P., Gregory A., Vázquez-Ortega A. (2019). Mapping Invasive Phragmites australis in the Old Woman Creek Estuary Using UAV Remote Sensing and Machine Learning Classifiers. Remote Sens., 11 (11), p.1380.

Aguilera A. G., Alpert P., Dukes J. S., Harrington, R. (2010). Impacts of the invasive plant Fallopia japonica (Houtt.) on plant communities and ecosystem processes. Biol. Invasions, 12 (5), pp. 1243-1252.

Akbani R., Kwek S., Japkowicz N. (2004). Applying Support Vector Machines to Imbalanced Datasets. In J.-F. Boulicaut, F. Esposito, F. Giannotti, D. Pedreschi (Éds.), Mach. Learn. : ECML 2004, 3201, pp. 39-50.

Ambroise C., McLachlan, G. J. (2002). Selection bias in gene extraction on the basis of microarray gene-expression data. Proc. Natl. Acad. Sci. U.S.A., 99 (10), pp. 6562-6566.

Asner G. P., Jones M. O., Martin R. E., Knapp D. E., Hughes R. F. (2008). Remote sensing of native and invasive species in Hawaiian forests. Remote Sens. Environ., 112 (5), pp. 1912-1926.

Barney J. N., Tharayil N., DiTommaso A., Bhowmik, P. C. (2006). The Biology of Invasive Alien Plants in Canada. 5. Polygonum cuspidatum Sieb. and Zucc. [= Fallopia japonica (Houtt.) Ronse Decr.]. Can. J. Plant. Sci., 86 (3), pp. 887-906.

Bashir S. M. A., Wang Y., Khan M., Niu Y. (2021). A comprehensive review of deep learning-based single image super-resolution. PeerJ Comput. Sci., 7, p. e621.

Belfiore O. R., Meneghini C., Parente, C., Santamaria, R. (2016). Application of different Pan-sharpening methods on WorldView-3 images. ARPN J. Eng. Appl. Sci., 11 (7). pp. 490-496

Benediktsson J. A., Sveinsson J. R. (1997). Feature extraction for multisource data classification with artificial neural networks. Int. J. Remote Sens., 18 (4), pp.727-740.

Bilgin G., Erturk S., Yildirim T. (2011). Segmentation of Hyperspectral Images via Subtractive Clustering and Cluster Validation Using One-Class Support Vector Machines. IEEE Trans. Geosci. Remote Sens., 49 (8), pp. 2936-2944.

Blagus R., Lusa L. (2013). SMOTE for high-dimensional class-imbalanced data. BMC bioinformatics, 14 (1), p.106.

Breiman L. (2001) Random forests. Mach. Learn., 45 (1), pp. 5-32.

Carlson T. N., Ripley D. A. (1997). On the relation between NDVI, fractional vegetation cover, and leaf area index. Remote Sens. Environ., 62 (3), pp. 241-252.

Castro-Esau K., Sánchez-Azofeifa G. A., Caelli T. (2004). Discrimination of lianas and trees with leaf-level hyperspectral data. Remote Sens Environ, 90 (3), pp.353-372.

Chaudhary P., Chaudhari A. K., Cheeran D. A. N., Godara S. (2012). Color Transform Based Approach for Disease Spot Detection on Plant Leaf. Int. J. Comput. Sci. Appl., 3 (6): pp. 65-70

Chen G., Zhao K., Powers R. (2014). Assessment of the image misregistration effects on object-based change detection. ISPRS J. Photogramm. Remote Sens., 87, pp. 19-27.

Chen M., Ke Y., Bai J., Li P., Lyu M., Gong Z., Zhou, D. (2020). Monitoring early stage invasion of exotic Spartina alterniflora using deep-learning super-resolution techniques based on multisource high-resolution satellite imagery: A case study in the Yellow River Delta, China. Int. J Appl. Earth. Obs. Geoinf., 92, p. 102180.

City of Québec. (2006). Plan directeur des milieux naturels et de la forêt urbaine. Rapport. 119p.

Cohen J. (1960). A Coefficient of Agreement for Nominal Scales. Educ. Psychol. Meas., 20 (1), pp. 37-46.

Collingham Y. C., Wadsworth R. A., Huntley B., Hulme P. E. (2000). Predicting the spatial distribution of non-indigenous riparian weeds : Issues of spatial scale and extent. J. Appl. Ecol., 37 (s1), pp. 13-27.

Congalton R. G. (1991). A review of assessing the accuracy of classifications of remotely sensed data. Remote Sens. Environ., 37 (1), pp. 35-46.

Costa M. V. C. V. da, Carvalho O. L. F. de, Orlandi A. G., Hirata I., Albuquerque A. O. de, Silva F. V. e, Guimarães R. F., Gomes R. A. T.Júnior, O. A. de C. (2021). Remote Sensing for Monitoring Photovoltaic Solar Plants in Brazil Using Deep Semantic Segmentation. Energies, 14 (10), p. 2960.

Dash J. P., Watt M. S., Paul T. S. H., Morgenroth J., Pearse G. D. (2019). Early Detection of Invasive Exotic Trees Using UAV and Manned Aircraft Multispectral and LiDAR Data. Remote Sens., 11 (15), pp.1812.

Dorigo W., Lucieer A., Podobnikar T., Čarni A. (2012). Mapping invasive Fallopia japonica by combined spectral, spatial, and temporal analysis of digital orthophotos. Int. J. Appl. Earth. Obs. Geoinf., 19, pp. 185-195.

Drăguţ L., Csillik O., Eisank C., Tiede D. (2014). Automated parameterisation for multi-scale image segmentation on multiple layers. ISPRS J. Photogramm. Remote Sens., 88, pp. 119-127.

Drăguţ L., Tiede D., Levick S. R. (2010). ESP : A tool to estimate scale parameter for multiresolution image segmentation of remotely sensed data. Int. J. Geogr. Inf. Sci., 24 (6), pp. 859-871.

Early R., Bradley B. A., Dukes J. S., Lawler J. J., Olden J. D., Blumenthal D. M., Gonzalez P., Grosholz E. D., Ibañez I., Miller L. P., Sorte C. J. B., Tatem A. J. (2016). Global threats from invasive alien species in the twenty-first century and national response capacities. Nat. Commun., 7 (1), p. 12485.

Escadafal R., Huete A. (1991). Etude des propriétés spectrales des sols arides appliquée à l'amélioration des indices de végétation obtenus par télédétection. Comptes rendus de l'Académie des sciences. Série 2, Mécanique, Physique, Chimie, Sciences de l'univers, Sciences de la Terre, 312 (11), pp. 1385-1391.

Ewald M., Skowronek S., Aerts R., Lenoir J., Feilhauer H., Van De Kerchove R., Honnay O., Somers B., Garzón-López C. X., Rocchini D., Schmidtlein S. (2020). Assessing the impact of an invasive bryophyte on plant species richness using high resolution imaging spectroscopy. Ecol. Indic., 110, p.105882.

Fernandes M. R., Aguiar F. C., Silva J. M. N., Ferreira M. T., Pereira J. M. C. (2014). Optimal attributes for the object based detection of giant reed in riparian habitats : A comparative study between Airborne High Spatial Resolution and WorldView-2 imagery. Int. J. Appl. Earth Obs. Geoinf., 32, pp. 79-91.

Fernandez A., Garcia S., Herrera F., Chawla, N. V. (2018). SMOTE for Learning from Imbalanced Data : Progress and Challenges, Marking the 15-year Anniversary. J. Artif. Intell. Res., 61, pp. 863-905.

Gašparović M., Dobrinić D. (2020). Comparative Assessment of Machine Learning Methods for Urban Vegetation Mapping Using Multitemporal Sentinel-1 Imagery. Remote Sens, 12 (12), p. 1952.

Gitelson A. A., Kaufman, Y. J. Stark, R., Rundquist D. (2002). Novel algorithms for remote estimation of vegetation fraction. Remote Sens. Environ, 80 (1), pp. 76-87.

Gong Y., Liao P., Zhang X., Zhang L., Chen G., Zhu K., ..., Lv Z. (2021). Enlighten-GAN for Super Resolution Reconstruction in Mid-Resolution Remote Sensing Images. Remote Sens., 13 (6), p. 1104.

Grizonnet M., Michel J., Poughon V., Inglada J., Savinaud M., Cresson R. (2017). Orfeo ToolBox : Open source processing of remote sensing images. Open Geospatial Data, Software and Standards, 2(1), p.15.

Guenther N., Schonlau, M. (2016). Support Vector Machines. Stata J.: Promoting Communications on Statistics and Stata, 16 (4), pp. 917-937.

Guido A., Pillar, V. D. (2017). Invasive plant removal : Assessing community impact and recovery from invasion. J. Appl. Ecol., 54 (4), pp. 1230-1237.

Guyon I., Weston J., Barnhill S. (2002). Gene Selection for Cancer Classification using Support Vector Machines. Mach. Learn., 46 (1): 389 - 422.

Hantson W., Kooistra L., Slim P. A. (2012). Mapping invasive woody species in coastal dunes in the Netherlands : A remote sensing approach using LIDAR and high-resolution aerial photographs. Appl. Veg. Sci., 15 (4), pp. 536-547.

Haralick R. M. (1979). Statistical and structural approaches to texture. Proc. IEEE., 67 (5), pp. 786-804.

Hirayama H., Sharma R. C., Tomita M., Hara, K. (2019). Evaluating multiple classifier system for the reduction of salt-and-pepper noise in the classification of very-high-resolution satellite images. Int. J. Remote Sens., 40 (7), pp. 2542-2557.

IUCN Council (2000). "Guidelines for the prevention of biodiversity loss caused by alien invasive species." in prepared by IUCN SSC invasive species specialist group (ISSG) approved by 51st meeting IUCN council gland SWITZERLAND, 1, pp. 12–25.

Jones D., Pike S., Thomas M., Murphy D. (2011). Object-Based Image Analysis for Detection of Japanese Knotweed s.l. Taxa (Polygonaceae) in Wales (UK). Remote Sens., 3 (2), 319-342.

Kattenborn T., Lopatin J., Förster M., Braun A. C., Fassnacht F. E. (2019). UAV data as alternative to field sampling to map woody invasive species based on combined Sentinel-1 and Sentinel-2 data. Remote Sens. Environ., 227, pp. 61-73.

Kavzoglu T., Mather P. M. (2004). The use of backpropagating artificial neural networks in land cover classification. Int. J. Remote Sens., 24 (23), pp. 4907-4938. h

Kazmi J. H., Haase D., Shahza A., Shaikh S., Zaidi S. M., Qureshi S. (2021). Mapping spatial distribution of invasive alien species through satellite remote sensing in Karachi, Pakistan : An urban ecological perspective. Int. J. Environ. Sci. Technol., 19 (5), pp. 3637-3654.

Kelsch A., Takahashi Y., Dasgupta R., Mader A. D., Johnson B. A., Kumar P. (2020). Invasive alien species and local communities in socio-ecological production landscapes and seascapes : A systematic review and analysis. Environ. Sci. Policy., 112, pp. 275-281.

Kermad C., Chehdi, K. (2000). Multi-bands image segmentation: A scalar approach. Proceedings 2000 International Conference on Image Processing (Cat. No.00CH37101), pp. 468-471.

Labonté J., Drolet G., Sylvain J.-D., Thiffault N., Hébert F., Girard, F. (2020). Phenology-Based Mapping of an Alien Invasive Species Using Time Series of Multispectral Satellite Data: A Case-Study with Glossy Buckthorn in Québec, Canada. Remote Sens., 12 (6), p. 922.

Langmaier M., Lapin, K. (2020). A Systematic Review of the Impact of Invasive Alien Plants on Forest Regeneration in European Temperate Forests. Front. Plant. Sci., 11, p. 524969.

Lantz N. J., Wang J. (2013). Object-based classification of Worldview-2 imagery for mapping invasive common reed, Phragmites aust. Can. J. Remote Sens., 39 (4), pp. 328-340.

Lass L. W., Prather T. S., Glenn N. F., Weber K. T., Mundt J. T., Pettingill J. (2005). A review of remote sensing of invasive weeds and example of the early detection of spotted knapweed (Centaurea maculosa) and babysbreath (Gypsophila paniculata) with a hyperspectral sensor. Weed Sci., 53 (2), pp.242-251.

Lavoie C., Guay G., Joerin F. (2014). Une liste des plantes vasculaires exotiques nuisibles du Québec : Nouvelle approche pour la sélection des espèces et l'aide à la décision. Écoscience, 21 (2), pp. 133-156.

Latte N., Lejeune P. (2020). PlanetScope radiometric normalization and sentinel-2 super-resolution (2.5 m): A straightforward spectral-spatial fusion of multi-satellite multi-sensor images using residual convolutional neural networks. Remote Sens., 12(15), p. 2366.

Lawrence R. L., Wood S. D., Sheley R. L. (2006). Mapping invasive plants using hyperspectral imagery and Breiman Cutler classifications (randomForest). Remote Sens. Environ., 100 (3), pp. 356-362.

Lemnaru C., Potolea R. (2012). Imbalanced Classification Problems: Systematic Study, Issues and Best Practices. In R. Zhang, J. Zhang, Z. Zhang, J. Filipe, and J. Cordeiro (Éds.), Enterp. Inf. Syst., 102, pp. 35-50.

Leonard L. A., Wren P. A., Beavers R. L. (2002). Flow dynamics and sedimentation in Spartina alterniflora and Phragmites australis marshes of the Chesapeake Bay. Wetlands, 22 (2), 415-424.

Li H., Jing L., Tang Y. (2017). Assessment of Pansharpening Methods Applied to WorldView-2 Imagery Fusion. Sens., 17(1), p. 89.

Lin C.-T., Hsieh T.-Y., Liu Y.-T., Lin Y.-Y., Fang C.-N., Wang Y.-K., Yen G., Pal N. R., Chuang C.-H. (2018). Minority Oversampling in Kernel Adaptive Subspaces for Class Imbalanced Datasets. IEEE Trans. Knowl. Data Eng., 30 (5), pp. 950-962.

Lu D., Weng Q. (2007). A survey of image classification methods and techniques for improving classification performance. Int. J. Remote Sens., 28 (5), pp. 823-870.

Martin F.-M., Müllerová J., Borgniet L., Dommanget F., Breton V., Evette A. (2018). Using Single- and Multi-Date UAV and Satellite Imagery to Accurately Monitor Invasive Knotweed Species. Remote Sens., 10 (10), p.1662.

Masse A. (2013). Développement et automatisation de méthodes de classification à partir de séries temporelles d'images de télédétection - Application aux changements d'occupation des sols et à l'estimation du bilan carbone. PhD.diss., Université Toulouse III Paul Sabatier, p. 190.

Massetti A., Sequeira M. M., Pupo A., Figueiredo A., Guiomar N., Gil A. (2016). Assessing the effectiveness of RapidEye multispectral imagery for vegetation mapping in Madeira Island (Portugal). Eur. J. Remote Sens., 49 (1), pp. 643-672.

Mhangara P., Mapurisa W., Mudau N. (2020). Comparison of Image Fusion Techniques Using Satellite Pour l'Observation de la Terre (SPOT) 6 Satellite Imagery. Applied Sciences, 10 (5), p. 1881.

Michez A., Piégay H., Jonathan L., Claessens H., Lejeune P. (2016). Mapping of riparian invasive species with supervised classification of Unmanned Aerial System (UAS) imagery. Int. J. Appl. Earth Obs. Geoinf., 44, pp. 88-94.

Monserud R. A. (1990). Methods for comparing global vegetation maps. WP-90-40, IIASA, Laxenburg.

More A. S., Rana, D. P. (2017). Review of random forest classification techniques to resolve data imbalance. 2017 1st International Conference on Intelligent Systems and Information Management (ICISIM), pp. 72-78.

Müllerová J., Bartaloš T., Brůna J., Dvořák P., Vítková M. (2017). Unmanned aircraft in nature conservation: An example from plant invasions. Int. J. Remote Sens., 38 (8-10), pp. 2177-2198.

Müllerová J., Pyšek P., Jarošík V., Pergl J. (2005). Aerial photographs as a tool for assessing the regional dynamics of the invasive plant species Heracleum mantegazzianum : Regional dynamics of H. mantegazzianum invasion. J. Appl. Ecol., 42 (6), pp. 1042-1053.

Müller M. U., Ekhtiari N., Almeida R. M., Rieke C. (2020). Super-resolution of multispectral satellite images using convolutional neural networks. In ISPRS Ann. Photogramm. Remote Sens. Spat. Inf. Sci. (ISPRS, 2020), pp. 33-40.

Nguyen H. M., Cooper, E. W., Kamei K. (2011). Borderline over-sampling for imbalanced data classification. Int. J. Knowl. Eng. Soft Data Paradig., 3 (1), p. 4.

Niphadkar M. (2016). Remote sensing of invasive plants: Incorporating functional traits into the picture. Int. J. Remote Sens., 37 (13), pp. 3074 - 3085.

Oktorini Y., Darlis V. V., Wahidin N., Jhonnerie R. (2021). The Use of SPOT 6 and RapidEye Imageries for Mangrove Mapping in the Kembung River, Bengkalis Island, Indonesia. IOP Conf. Ser. Earth Environ. Sci., 695 (1), p. 012009.

Page N. A., Wall R. E., Darbyshire S. J., Mulligan G. A. (2006). The Biology of Invasive Alien Plants in Canada. 4. Heracleum mantegazzianum Sommier and Levier. Can. J. Plant. Sci., 86 (2), pp. 569-589.

Park H., Kim N., Park S., Choi J. (2020). Sharpening of Worldview-3 Satellite Images by Generating Optimal High-Spatial-Resolution Images. Appl. Sci., 10 (20), p. 7313.

Patil A., Framewala A., Kazi, F. (2020). Explainability of SMOTE Based Oversampling for Imbalanced Dataset Problems. 2020 3rd International Conference on Information and Computer Technologies (ICICT), pp. 41-45.

Paz-Kagan T., Silver M., Panov N., Karnieli A. (2019). Multispectral Approach for Identifying Invasive Plant Species Based on Flowering Phenology Characteristics. Remote Sens., 11 (8), p. 953.

Poulin B., Davranche A., Lefebvre G. (2010). Ecological assessment of Phragmites australis wetlands using multi-season SPOT-5 scenes. Remote Sens. Environ., 114 (7), pp. 1602-1609.

Pouliot D., Latifovic R., Pasher J., Duffe J. (2018). Landsat super-resolution enhancement using convolution neural networks and Sentinel-2 for training. Remote Sens., 10 (3), p. 394.

Pranto A. S., Paul, M. K. (2021). Performance Analysis of Ensemble Based Approaches to Mitigate Class Imbalance Problem after Applying Normalization. 2021 International Conference on Automation, Control and Mechatronics for Industry 4.0 (ACMI), pp. 1-5.

Qian W., Huang Y., Liu Q., Fan W., Sun Z., Dong H., Wan F., Qiao X. (2020). UAV and a deep convolutional neural network for monitoring invasive alien plants in the wild. Comput. Electron. Agric., 174, p.105519.

Ranchin T., Aiazzi B., Alparone L., Baronti S., Wald L. (2003). Image fusion. The ARSIS concept and some successful implementation schemes. ISPRS J. Photogramm. Remote Sens., 58 (1-2), pp. 4-18.

R Core Team (2021). A language and environment for statistical computing. R Foundation for Statistical Computing, Vienna, Austria.URL https://www.R-project.org/.

Richhariya B., Tanveer, M. (2020). A reduced universum twin support vector machine for class imbalance learning. Pattern Recognit., 102, p. 107150.

Roy H. E., Bacher S., Essl F., Adriaens T., Aldridge D. C., Bishop J. D. D., Blackburn T. M., Branquart E., Brodie J., Carboneras C., Cottier-Cook E. J., Copp G. H., Dean H. J., Eilenberg J., Gallardo B., Garcia M., García-Berthou E., Genovesi P., Hulme P. E., … Rabitsch W. (2019). Developing a list of invasive alien species likely to threaten biodiversity and ecosystems in the European Union. Glob. Chang. Biol., 25 (3), pp. 1032-1048.

Royimani L., Mutanga O., Odindi J., Dube T., Matongera T. N. (2019). Advancements in satellite remote sensing for mapping and monitoring of alien invasive plant species (AIPs). Phys. Chem. Earth (2002), Parts A/B/C, 112, pp. 237-245.

Rupasinghe P. A., Chow-Fraser P. (2019). Identification of most spectrally distinguishable phenological stage of invasive Phramites australis in Lake Erie wetlands (Canada) for accurate mapping using multispectral satellite imagery. Wetl. Ecol. Manag., 27 (4), pp. 513-538.

Rupasinghe P. A., Chow-Fraser P. (2021). Mapping Phragmites cover using WorldView 2/3 and Sentinel 2 images at Lake Erie Wetlands, Canada. Biol. Invasions, 23 (4), pp. 1231-1247.

Samat A., Li E., Wang W., Liu S., Lin C., Abuduwaili J. (2020). Meta-XGBoost for Hyperspectral Image Classification Using Extended MSER-Guided Morphological Profiles. Remote Sens., 12 (12), p.1973.

Sánchez-Azofeifa G. A., Castro K., Wright S. J., Gamon J., Kalacska M., Rivard B., Schnitzer S. A., Feng J. L. (2009). Differences in leaf traits, leaf internal structure, and spectral reflectance between two communities of lianas and trees : Implications for remote sensing in tropical environments. Remote Sens. Environ., 113 (10), pp. 2076-2088.

Shackleton R. T., Biggs R., Richardson D. M., Larson B. M. H. (2018). Social-ecological drivers and impacts of invasion-related regime shifts : Consequences for ecosystem services and human wellbeing. Environ. Sci. Policy, 89, pp. 300-314.

Shermeyer J., Van Etten A. (2019). The effects of super-resolution on object detection performance in satellite imagery. In Proceedings of the IEEE/CVF Conference on Computer Vision and Pattern Recognition Workshop.

Singh K. K., Chen Y.-H., Smart L., Gray J., Meentemeyer, R. K. (2018). Intra-annual phenology for detecting understory plant invasion in urban forests. ISPRS J. Photogramm. Remote Sens., 142, pp. 151-161.

Ustin S. L., DiPietro D., Olmstead K., Underwood E., Scheer G. J. (2002). Hyperspectral remote sensing for invasive species detection and mapping. IEEE Int. Geosci. Remote Sens. Symp. Proc., 3, pp. 1658-1660.

Varin M., Chalghaf B., Joanisse G. (2020). Object-Based Approach Using Very High Spatial Resolution 16-Band WorldView-3 and LiDAR Data for Tree Species Classification in a Broadleaf Forest in Quebec, Canada. Remote Sens., 12 (18), p. 3092.

Varin M, Allostry J., Chalghaf B. 2020. Caractérisation et suivi des écosystèmes riverains de l'agglomération de Québec - volet 1 caractérisation des écosystèmes riverains. Centre d'enseignement et de recherche en foresterie de Sainte-Foy inc. (CERFO). Rapport 2019-14. 24 pages.

Wang Y., Bashir S. M. A., Khan M., Ullah Q., Wang R., Song Y., ... ,Niu Y. (2022). Remote sensing image super-resolution and object detection: Benchmark and state of the art. Expert Syst Appl, p. 116793.

Waser L., Küchler M., Jütte K., Stampfer T. (2014). Evaluating the Potential of WorldView-2 Data to Classify Tree Species and Different Levels of Ash Mortality. Remote Sens., 6 (5), pp. 4515-4545.

Xu X., Chen W., Sun Y. (2019). Over-sampling algorithm for imbalanced data classification. JSEE, 30 (6), pp. 1182-1191.

Yang L., Mansaray L., Huang J., Wang L. (2019). Optimal Segmentation Scale Parameter, Feature Subset and Classification Algorithm for Geographic Object-Based Crop Recognition Using Multisource Satellite Imagery. Remote Sens., 11 (5), p. 514.

Yang Y. (2001). A study of thresholding strategies for text categorization. Proceedings of the 24th Annual International ACM SIGIR Conference on Research and Development in Information Retrieval - SIGIR '01, pp. 137-145.

Zarei A., Hasanlou M., Mahdianpari M. (2021). A comparison of machine learning models for soil salinity estimation using multi-spectral earth observation data. ISPRS Ann. Photogramm. Remote Sens. Spat. Inf. Sci., V-3-2021, pp. 257-263.

Zhang Y. (2004). Understanding Image Fusion. Photogramm Eng Remote Sensing, 70 (6), pp. 657-661

Zhao Z., Peng H., Lan C., Zheng Y., Fang L., Li J. (2018). Imbalance learning for the prediction of N6-Methylation sites in mRNAs. BMC Genomics, 19 (1), p. 574.

Zhou Y., Zhang R., Wang S., Wang F. (2018). Feature Selection Method Based on High-Resolution Remote Sensing Images and the Effect of Sensitive Features on Classification Accuracy. Sens., 18 (7), p. 2013.

Zhou Q., Zhang X., Yu L., Ren L., Luo Y. (2021). Combining WV-2 images and tree physiological factors to detect damage stages of Populus gansuensis by Asian longhorned beetle (Anoplophora glabripennis) at the tree level. For. Ecosyst., 8 (1), pp. 1-12.

5. Cartographie des nerpruns bourdaine et cathartique (*Frangula alnus* and *Rhamnus cathartica*) en utilisant les images satellitaires multi-date SPOT-7, WorldView-3 et GeoEye-1

L'article scientifique présentant les résultats de cette étude a été soumis au journal scientifique *International Journal of Digital Earth***,** le 08 Août 2022 (preuve de soumission : annexe 2). La numérotation des titres, figures, tableaux et annexes a été modifiée afin de faciliter la lecture.

Mapping common and glossy buckthorns (*Frangula alnus* and *Rhamnus cathartica*) using multi-date satellite imagery WorldView-3, GeoEye-1 and SPOT-7.

Nininahazwe Fiston[a,b,c*], Mathieu Varin[b] and Jérôme Théau[a,c]
[a]*Département de Géomatique appliquée, Université de Sherbrooke, Sherbrooke, Canada;*
[b]*Centre d'enseignement et de recherche en foresterie (CERFO), Québec, Canada*
[c]*Centre de la science de la biodiversité du Québec, 1205 Av. du Docteur-Penfield S3/18, Montréal, Canada*

**Corresponding author Email : Fiston.nininahazwe@usherbrooke.ca*

Abstract :

Buckthorns (Glossy buckthorn, *Frangula alnus* and common buckthorn, *Rhamnus cathartica*) represent a threat to biodiversity as their high competitivity lead to native species' replacement and the inhibition of forest regeneration. Early detection strategies are therefore necessary to limit impacts, and remote sensing is one of the techniques for early invasion detection. Few studies have used phenological remote sensing approaches to map buckthorn distribution from medium spatial resolution images. Those studies highlighted the difficulty of detecting buckthorns of low density and in understory using this category of images. The main objective of this study was to develop an approach using multi-date very high spatial resolution satellite imagery to map buckthorns in the understory and at low density in the Québec city area. We used WorldView-3, GeoEye-1 and SPOT-7 satellite imagery and machine learning classifiers (Support Vector Machines, Random Forest and Extreme Gradient Boosting). The multi-date classification performed well using a RF classifier (Kappa = 0.72, overall accuracy = 83%). We achieved better performances than previous studies carried out in similar environments. However, buckthorns in understory distribution was identified as the main limit to this approach, and LiDAR data could be used to improve buckthorn mapping in similar environments.

Keywords : Invasive alien plant species, *Frangula alnus*, *Rhamnus cathartica,* remote sensing, buckthorn, multi-date satellite imagery, machine learning.

5.1. Introduction

Human activities and climatic variability are the main drivers for the introduction and spread of invasive alien plant species (IAPS) (Kumar Rai and Singh, 2020; Langmaier and Lapin, 2020; Paz-Kagan *et al.,* 2019; Guido and Pillar, 2017; Early *et al.,* 2016). This introduction, intentional or accidental, as well as its spread after installation, can lead to ecological, health and negative economic impacts (e.g., the replacement of native species, the expense of eradication interventions, the loss of invaded land value, photodermatitis from contact with the plant sap of some IAPS such as giant hogweed (*Heracleum mantegazzianum*)) (Lavoie *et al.,* 2014; Vilà *et al.,* 2010; Mack *et al.,* 2000).

Glossy buckthorn (*Frangula alnus*) and common buckthorn (*Rhamnus cathartica*) are native to Europe and were introduced in North America in the early 19th century, initially used as windbreaks (Boettcher, Gautam, and Cook, 2021; Becker *et al.,* 2013; Heneghan *et al.,* 2006). These IAPs colonize open environments (e.g., wastelands) where they form very dense colonies (Heneghan *et al.,* 2006; Frapier, 2004), forest edges, understory and along rivers (Lavoie *et al.,* 2014). These IAPS are also characterized by a particular phenology. Their leaves remain green late in the fall and appear very early in the spring (Labonté *et al.,* 2020; Becker *et al.,* 2013; Knight *et al.,* 2007; Archibold *et al.,* 1997). Heneghan *et al.* (2006) also found that buckthorns alter soil chemical properties as a result of altered moisture and accelerated organic matter transformation processes (e.g. nitrogen and carbon mineralization). These changes in organic matter cycling can subsequently cause an increase in pH and decrease of soil nutrient availability for other organisms (Knight *et al.,* 2007). The loss of biodiversity, the facilitation of the establishment of new invasive species and the inhibition of forest regeneration are the main impacts of these IAPS in invaded areas (Lavoie *et al.,* 2014; Knight *et al.,* 2007; Frapier, 2004).

Buckthorns are more competitive and replace native species by reducing their recruitment. As an example, Frapier (2004) showed that sites with high buckthorn percentage cover (> 90% cover), recruited fewer new pines (0.11 seedlings/m^2) than sites without buckthorns (0.40 seedlings/m^2) in a coniferous forest (*Pinus* sp.) of New Hampshire (USA). Replacement of native species is also facilitated by the high germination rate of buckthorns, which can reach 85% (Archibold *et al.,* 1997). Moreover, their high photosynthesis rate can be up to twice that of native species which

allows them to grow very rapidly (Kalkman *et al.,* 2019; Harrington *et al.,* 1989). This high competitiveness (Boettcher *et al.,* 2021; Kalkman *et al.,* 2019) requires early detection strategies so that eradication interventions can be performed at the early stages of invasion. Identification can be made by *in situ* inventories which are time consuming and expensive, especially when conducted in areas with limited access (Lawrence *et al.,* 2006). Remote sensing has the potential to reduce these constraints and improve detection.

Only two studies that used remote sensing to map buckthorn distribution were found in the literature. A phenological approach based on a series of six multi-date (April, June, August, September, October and November) Landsat-8 OLI images was used by Labonté *et al.* (2020) to map understory buckthorns in Richmond and Cookshire (Quebec, Canada), in a forest dominated by broadleaf deciduous and coniferous trees. A relatively low overall accuracy of 69% was obtained and attributed to low levels of buckthorn cover and spectral mixing in the images (Labonté *et al.,* 2020). Becker *et al.* (2013) used the same approach with a series of 49 Landsat 7 ETM+ and Landsat 5 TM images (January to December between 2001 and 2011) in Ohio and Michigan (USA) and obtained an overall accuracy of 88%. This good accuracy can be explained by the study environment (oak openings) and high buckthorn density. Labonté *et al.* (2020) showed that the classification error decreased with the increase of buckthorn cover levels in the studied plots (plot size = 30 × 30 m), as the spectral mixing in the pixel is reduced. For example, this error was 20% when buckthorn cover was greater than or equal to 75%, and 31% with cover greater than or equal to 25%. These studies thus highlight the limits of detecting low density and understory buckthorns (i.e., low percentage cover in a pixel) using medium spatial resolution satellite imagery. Although the use of multi-date very high (VHR) and high spatial resolution (HR) images could improve classification accuracy (Labonté *et al.,* 2020; Becker *et al.,* 2013), there are no studies to date that have incorporated these data to map low-density and understory buckthorns.

The main objective of this study is then to explore and compare the use of multi-date HR and VHR satellite imagery in combination with machine learning classifiers to detect understory buckthorns at low density.

5.2. Material and methods

5.2.1. Study area

The study area is a 4 km long riparian zone located along the Beauport River in Quebec City (46°52'02"N, 71°12'35"W) (Figure 7). The canopy of the area is dominated by broadleaf deciduous trees: boxelder maple (*Acer negundo*), red maple (*Acer rubrum*), American elm (*Ulmus americana*), black willow (*Salix nigra*) and white birch (*Betula papyrifera*). A few patches of evergreen trees are present, mainly coniferous including blue spruce (*Picea pungens*) and balsam fir (*Abies balsamea*). In this area, buckthorn individuals are understory and isolated and do not form homogeneous patches. We therefore chose this riparian zone as our study area because of (1) the presence of many buckthorn individuals and (2) their spatial distribution (i.e. low density and understory) allowing us to test the detection efficiency of the VHR and HR images.

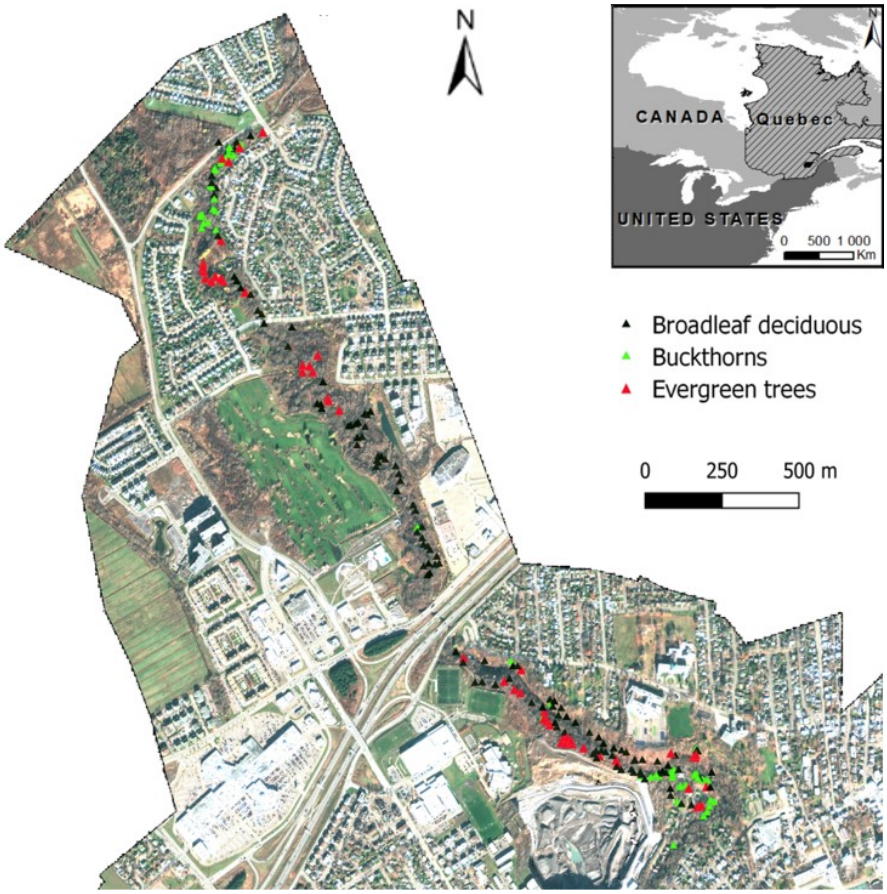

Figure 7 : Study area and collected sample locations. The background is a true color composite (red, green, blue) of a GeoEye-1 satellite image acquired on November 5th 2020.

5.2.2. Reference data

Reference data collection was conducted in the field during two periods: in the summer (June 26 to August 26, 2020) and in late fall (October 15 to 21, 2021), when buckthorns are easily identifiable after most broadleaf deciduous have lost their leaves (Figure 8). Three classes of reference data were collected: buckthorn, evergreen, and broadleaf deciduous species. Two high-accuracy (≈1m) Pro 6 H (Trimble, California) and Arrow Gold (EOS positioning system, Quebec) GNSS (Global Navigation Satellite Systems) receivers were used to locate and record the crown centre position of individuals of the three classes.

The broadleaf deciduous class corresponds to the dominant individuals in the study area and samples were randomly collected. Buckthorn and evergreen species were less numerous, and all accessible individuals were collected. Buckthorns that were less than 4 m tall or characterized by small crown surface were not used, as they are completely understory and could not be detected by remote sensing. The total number of points collected for each class was 54, 50, and 108 for buckthorn, evergreen and deciduous species, respectively.

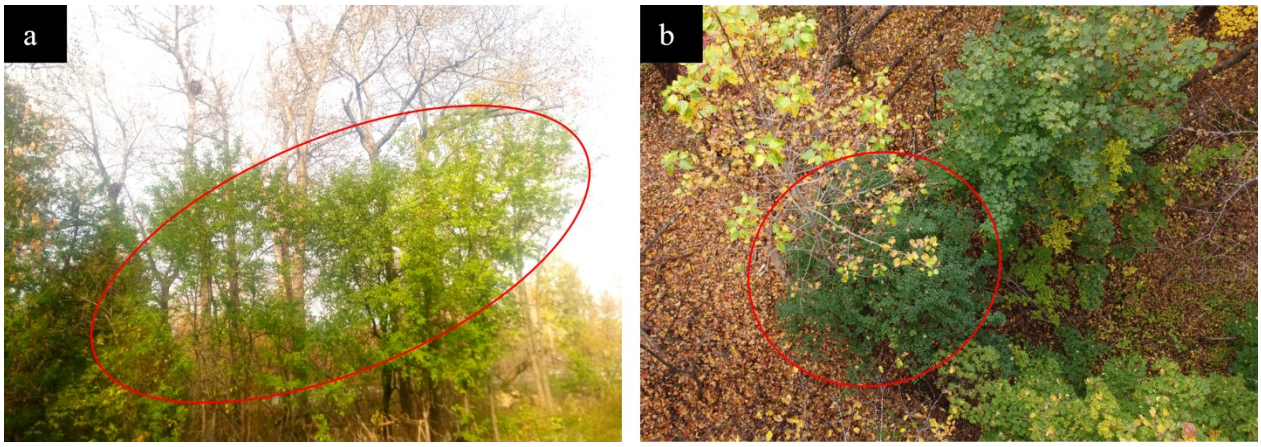

Figure 8 : (a) Field (October 20, 2021) and (b) drone (October 15, 2021) photos of Buckthorns (red circles) understory (source: Centre d'enseignement et de recherche en foresterie).

5.2.3. Images acquisition and pre-processing

Three multi-source images acquired by WV-3/WV110 (WorldView-3 /World View 110 camera, July 07, 2020), SPOT-7/NAOMI (Satellite Pour l'Observation de la Terre -7, New AstroSat Optical Modular Instrument, October 26, 2019), and GeoEye-1/GIS (GeoEye Imaging System, November 05, 2020) were used. The spectral and spatial characteristics of these images are presented in Table 7.

Table 7 : Imagery specifications

Satellite	Band	Wavelength range (center) (nm)	Spatial resolution (m)
WV-3	Coastal	400 – 450 (425)	1.24
	Blue	450 – 510 (480)	
	Green	510 – 580 (545)	
	Yellow	585 – 625 (605)	
	Red	630 – 690 (660)	
	Red Edge	705 – 745 (725)	
	Near-infrared	770 – 895 (832.5)	
	Near-infrared	860 – 1040 (950)	
	Panchromatic	450 – 800 (625)	0.31
SPOT-7	Blue	450 – 520 (485)	6
	Green	530 – 590 (560)	
	Red	625 – 695 (660)	
	Near-infrared	760 – 890 (825)	
	Panchromatic	450 – 745 (597.5)	1.5
GeoEye-1	Blue	450 – 510 (480)	2
	Green	510 – 580 (545)	
	Red	655 – 690 (672.5)	
	Near-infrared	780 – 920 (850)	
	Panchromatic	450 – 800 (625)	0.5

WV-3 : WorldView3, SPOT-7 : Satellite Pour l'Observation de la Terre -7

Atmospheric corrections were performed using the ATCOR module (PCI Geomatics 2018) and fusion of the panchromatic band with the multispectral bands was performed using the ratio component substitution (RCS) fusion method available in the Orfeo toolbox (Deur *et al.,* 2021; *et al.,* 2020; Grizonnet *et al.,* 2017).

A digital terrain model (Varin *et al.,* 2020) at one-meter spatial resolution was used for orthorectification of the pansharpened images, and an orthomosaic of the WV-3 image was generated using the Bundle colour balancing method (PCI Geomatics 2018) from fourteen tiles.

Three masks were applied to remove unvegetated areas, shadows and vegetation less than 4 m tall. A first mask was created using the WV-3 image to remove water, bare soil and buildings by applying a normalized difference vegetation index (NDVI) threshold (NDVI < 0.37) based on the NDVI distribution of the field reference data. A second mask to remove shadows was applied using a shadow index (SI) threshold (Zhou *et al.,* 2018) (SI ≤ 13.13) based on SI analysis of shadow objects. A third mask to remove vegetation below 4 m was applied using a digital height model at one-meter spatial resolution (Varin *et al.,* 2020).

5.2.4. Segmentation

The GeoEye-1 image was used for segmentation because of its acquisition period (i.e., fall) that maximizes the separability between buckthorns and other species (i.e., buckthorns leaves remain green late in the fall) and its better spatial resolution than the SPOT-7 image taken at the same season. The multi-resolution algorithm was selected for segmentation due to its performance in several recent image segmentation studies (Lourenço *et al.,* 2021; Chen *et al.,* 2021).

The segmentation parameter values (i.e., scale, colour, and compactness) were determined using an iterative trial-and-error process combined with the estimation of scale parameter (ESP2) method (Drăguţ *et al.,* 2014, Fernandes *et al.,* 2014; Müllerová *et al.,* 2013; Jones *et al.,* 2011, Drăguţ *et al.,* 2010). The values obtained are 5, 0.9 and 0.5, respectively for scale, colour, and compactness and 1 and 2 for the weight of the blue and green bands and of the red and near-infrared bands, respectively.

Spectral, textural, and geometric arithmetic features were extracted from the objects resulting from the segmentation (Table 8). A total of 150 features for WV-3 and 77 for each of the SPOT-7 and GeoEye-1 images were calculated, for a total of 304. The features were centred and scaled and a correlation analysis was performed to eliminate correlated features using a Pearson coefficient greater than or equal to 0.85 (Varin *et al.,* 2020). The Jeffries Matusita (JM) separability distance was used to select the most relevant features among two correlated ones.

Table 8 : Features used for classification

Category	Feature	Band combination	Reference
Spectral	Mean	All	
	Maximum	All	
	Standard deviation	All	
	95^{th} percentile	All	
	Skewness	All	
	NDVI (Normalized Difference Vegetation Index)	(NIR - red) / (NIR + RE)	Carlson et Ripley (1997)
	RENDVI (Red-Edge Normalized Difference Vegetation Index)	(NIR - RE) / (NIR + RE)	Waser *et al.,* (2014)
	VARI (Visible Atmospherically Resistant Index)	(green - red) / (green + red - blue)	Gitelson *et al.,* (2002)
	RGR (Red Green Ratio)	red / green	Zhou *et al.,* (2021)
	SR (Simple Ratio)	NIR /rouge	Zhou *et al.,* (2021)
	BTBR (Bi-Temporal Band Ratio)	red, green*	Dorigo *et al.,* (2012)
	HSI (Hue, Saturation, Intensity)	red, green, blue*	Chaudhary *et al.,* (2012)
	CI (Colour Index)	(red - green) / (red + green)	Escadafal *et al.,* (1991)
	BI (Brightness index)	$(red^2 + NIR^2)^{0.5}$	Zhou *et al., (*2018)
Textural	GLCM (Gray Level Co-occurrence Matrix): contrast, correlation, entropy, homogeneity, angular second moment, mean, standard deviation GLDV (Gray Level Difference Vector) : contrast, entropy, mean, angular second moment	All	Haralick (1979)
Geometric	Width, length, compactness	-	-

NIR : Near-infrared, RE : Red-Edge

*Because of limited space, only used bands are presented (see references for detailed definition)

5.2.5. Classification approach and optimization of machine learning classifiers

Object-based classification was performed following a multi-date approach by combining the three images and the BTBR (Bi-Temporal Band Ratio) (WV-3 + SPOT-7 + GeoEye-1 + BTBR). The BTBR (equation 1) developed by Dorigo *et al.* (2012) and used for multi-date classification was calculated between WV-3 and each of the other two images (BTBR1: WV-3 and GeoEye-1, BTBR2: WV-3 and SPOT-7),

$$\mathrm{BTBR} = \frac{\frac{R_{off}}{R_{on}} - \frac{G_{off}}{G_{on}}}{\frac{R_{off}}{R_{on}} + \frac{G_{off}}{G_{on}}} \quad (1)$$

where R and G indicate reflectance values in red and green band, respectively. The suffixes indicate the image acquisition period (growing season (on) and senescence period (off)). Random Forest (RF) (Breiman 2001), Support Vector Machines (SVM) (Guenther and Schonlau 2016) and Extreme Gradient Boosting (XGBoostt) (Zarei, Hasanlou, and Mahdianpari 2021; Samat *et al.,* 2020) classifiers were used for classification and the recursive feature elimination method was used to select relevant discriminant features (Yang *et al.,* 2019; Guyon *et al.,* 2002; Ambroise and McLachlan 2002). The caret library in R (R core team 2021) was used to optimize the number of random features used at each node (mtry) and the number of decision trees (ntree) for the RF classifier. The radial basis function was used for SVM; the cost and sigma parameters as well as the XGBoost parameters, such as the learning rate, were automatically optimized using the caret library (R core team 2021).

5.2.6. Classification accuracy assessment

The segments were overlaid on the reference data, and 70% of each class was used to train the models while 30% of the segments were used for validation. Cohen's Kappa coefficient (Congalton 1991; Cohen 1960), overall accuracy, and the F1-score (i.e., the harmonic mean of user and producer accuracy) (Costa *et al.,* 2021; Yang 2001) were used to evaluate the accuracy of the models. The output of the models is a membership probability between 0 and 1 for each class. The sum of the class probabilities is equal to 1. The membership of the object was the class with the highest probability.

5.3. Results and discussion

The multi-date classification performed in this study shows that the RF classifier performs better (Kappa = 0.72) compared to the other classifiers (Kappa = 0.69 (SVM); 0.66 (XGBoost) (Table 9).

Table 9 : Performance measures of classifiers. Values in bold indicate the maximum performance values

GeoEye-1 + WV-3 + SPOT-7 + BTBR1+ BTBR2				
		RF	SVM	XGBoost
Global	Kappa	**0.72**	0.69	0.66
	OA	**0.83**	0.82	0.80
Buckthorns	UA	0.67	0.67	0.67
	PA	0.57	0.43	0.43
	F1-score	0.62	0.52	0.52
Evergreen trees	UA	0.93	0.93	0.93
	PA	0.93	1.00	0.93
	F1-score	0.93	0.97	0.93
Broadleaf deciduous	UA	0.85	0.81	0.78
	PA	0.91	0.91	0.91
	F1-score	0.88	0.85	0.84
Mean F1-score		**0.81**	0.78	0.76
Standard deviation		0.13	0.17	0.16

BTBR: Bi-Temporal Band Ratio, BTBR1: WV-3 and GeoEye-1, BTBR2: WV-3 and GeoEye-1, RF: Random Forest, SVM: Support vector machines, XGBoost: Extreme gradient boosting, OA: Overall Accuracy, UA: User's accuracy, PA: Producer Accuracy.

For individual class performance, buckthorns are less well detected compared to the other classes regardless of the classifier used. In particular, the optimal classifier (RF) for buckthorns reaches 0.62 (F1-score) compared to 0.93 and 0.88 for broadleaf deciduous and evergreen species, respectively (Table 9). This low F1-score value results from omission errors (43%, 1-producer's accuracy) and commission errors (33%, 1 - user's accuracy). The omission errors indicate the difficulty of the classifier to predict some buckthorns, while the commission errors show that some absences (e.g., broadleaf deciduous or evergreen species) were classified as buckthorns. The spatial distribution of buckthorns in the study area probably explains these errors. Although individuals less than 4 m tall were eliminated from the analyses, buckthorns are always found below the canopy of other dominant broadleaf deciduous, so branches and trunks of other overhanging trees would contribute

strongly to the pixel reflectance (Labonté *et al.,* 2020). Broadleaf deciduous trees (e.g., black willow) were also observed with green leaves late in the fall, which could contribute to misclassification.

These results produced higher levels of accuracy (overall accuracy = 83%) compared to studies conducted in similar conditions (Labonté *et al.,* 2020) (overall accuracy = 69%). The relatively low performance of Labonte *et al.*'s study was related to the spectral mixing in the pixels of the medium spatial resolution image they used (Landsat 8 OLI), in a context where the size of the individuals was smaller than that of the pixels (Labonté *et al.,* 2020). The VHR used in our study therefore appear to have reduced the effects of spectral mixing. On the other hand, the results obtained here are comparable to those found by Becker, Zmijewski, and Crail (2013), who detected buckthorns in a more favourable context (i.e., open environment and high densities) than ours (OA: 88%, Kappa: 0.73). Considering the detection challenges in our study area, our multi-date classification approach is performing well, although improvements are needed to produce a more accurate map that can be used directly by managers.

In addition, fifteen features used by the optimal classifier highlight the relevance of the multi-date classification approach. The features calculated from the WV-3 and GeoEye-1 images contributed in similar proportions (6/15 for WV-3 and 7/15 for GeoEye-1), in addition to the BTBR calculated between these two images (BTBR1). However, the contribution of the features calculated from SPOT-7 is less significant (1/15). This could be due to the low spatial resolution of the multispectral SPOT-7 bands (6 m, before pansharpening) compared to those from GeoEye-1 (2 m) and WV-3 (1.24 m), hence the advantage of using VHR images in the development of buckthorn mapping methods. Our study also highlights the low relevance of adding lower resolution images to VHR images acquired at the same period.

In environments similar to our study area, the omission and commission errors could be reduced using other data sources, such as high-density point clouds from LiDAR (Light Detection and Ranging) acquired in the fall season. These data have not yet been exploited for buckthorn detection, although they have been used successfully in previous vegetation mapping studies (Budei *et al.,* 2018; Dalponte *et al.,* 2008; Asner *et al.,* 2008). In particular, high density or multiple-return LiDAR would allow to derive several structural features

(e.g., crown shape and area), identification of crowns at different heights (Shi *et al.,* 2018), and the extraction of several radiometric features derived from backscattered signal intensity (Shi *et al.,* 2018; Ørka *et al.,* 2009; Dalponte *et al.,* 2009; Dalponte *et al.,* 2008; Asner *et al.,* 2008). These features could be incorporated into optical images to improve remote sensing mapping approaches for buckthorns in understory and at low density. Features such as height could allow for a more accurate removal of unsuitable vegetation strata using a canopy height model (Asner *et al.,* 2008), while radiometric features could be used for discrimination between buckthorns and native species (Shi *et al.,* 2018; Ørka *et al.,* 2009; Dalponte *et al.,* 2008).

5.4. Conclusion

The performances of mapping buckthorns in understory at low density using multi-date VHR and HR images is satisfactory in comparison with similar but rare previous studies. However, the use of this approach in an operational context (e.g., target intervention areas) would require improvements to reduce the errors and thereby target the problematic areas more precisely. Future studies could incorporate LiDAR data as well as multispectral images at centimetre resolution (e.g., drone images) to improve buckthorn detection in understory.

5.5. Disclosure statement

Authors declare no conflict of interest

5.6. Acknowledgments

The authors gratefully acknowledge Nicolas Turcotte-Major (Québec city), Anne-Marie Dubois (CERFO), Camille Armellin (CERFO), Jean Marchal (CERFO), Julie Deslandes (Québec city) and Ramdani Mustapha (Québec city) for their support during the project.

5.7. Funding

This work was supported by the Mitacs Accélération program under grant (IT16759) and Québec city.

5.8. Data availability statement

Data that support the findings of this study are openly available in the Open Science Framework data repository.

5.9. References

Ambroise, C., and McLachlan, G. J. (2002). "Selection Bias in Gene Extraction on the Basis of Microarray Gene-expression Data." *Proceedings of the National Academy of Sciences 99*(10): 6562-6566. doi:https://doi.org/10.1073/pnas.102102699.

Archibold, O. W., Brooks, D., and Delanoy, L. (1997). "An Investigation of the Invasive Shrub European Buckthorn, Rhamnus cathartica L., near Saskatoon, Saskatchewan." *Canadian Field-Naturalist* 111(4): 617-621. https://www.researchgate.net/profile/Darin Brooks/publication/239951389_An_investigation_of_the_invasive_shrub_European_Buckthorn_Rhamnus_cathartica_L_near_Saskatoon_Saskatchewan/links/54621dd30cf2c1a63c0295e2/An-investigation-of-the-invasive-shrub-European-Buckthorn-Rhamnus-cathartica-L-near-Saskatoon-Saskatchewan.pdf

Asner, G. P., Knapp, D. E., Kennedy-Bowdoin, T., Jones, M. O., Martin, R. E., Boardman, J., and Hughes, R. F. (2008). "Invasive Species Detection in Hawaiian Rainforests Using Airborne Imaging Spectroscopy and LiDAR." *Remote Sensing of Environment* 112(5): 1942-1955. doi:https://doi.org/10.1016/j.rse.2007.11.016.

Becker, R. H., Zmijewski, K. A., and Crail, T. (2013). "Seeing the Forest for the Invasives : Mapping Buckthorn in the Oak Openings." *Biological Invasions* 15(2): 315-326. doi:https://doi.org/10.1007/s10530-012-0288-8

Boettcher, T. J., Gautam, S., and Cook, J. (2021). "The Impact of Invasive Buckthorn on Ecosystem Services and its Potential for Bioenergy Production : A Review." *Journal of Sustainable Forestry* 1-23. doi:https://doi.org/10.1080/10549811.2021.1992637.

Budei, B. C., St-Onge, B., Hopkinson, C., and Audet, F. A. (2018). "Identifying the Genus or Species of Individual Trees Using a Three-wavelength Airborne Lidar System." *Remote sensing of Environment* 204:632-647. doi:https://doi.org/10.1016/j.rse.2017.09.037.

Carlson, T. N., and Ripley, D. A. (1997). "On the Relation Between NDVI, Fractional Vegetation Cover, and Leaf Area Index." *Remote Sensing of Environment* 62(3): 241-252. doi:https://doi.org/10.1016/S0034-4257(97)00104-1.

Chaudhary, P., Chaudhari, A. K., Cheeran, A. N., and Godara, S. (2012). "Color Transform Based Approach for Disease Spot Detection on Plant Leaf. *International journal of computer science and telecommunications* 3(6): 65-70.

Chen, Y., Chen, Q., and Jing, C. (2021). "Multi-resolution Segmentation Parameters Optimization and Evaluation for VHR Remote Sensing Image Based on *Mean* NSQI and Discrepancy measure." *Journal of Spatial Science* 66(2): 253-278. doi: https://doi.org/10.1080/14498596.2019.1615011.

Cohen, J. (1960). "A Coefficient of Agreement for Nominal Scales." *Educational and Ps ychological Measurement* 20(1): 37-46. doi: https://doi.org/10.1177/00131644600 2000104.

Congalton, R. G. (1991). "A review of Assessing the Accuracy of Classifications of Remotely Sensed data." *Remote Sensing of Environment* 37(1): 35-46. doi:https:// doi.org/10.1016/0034-4257(91)90048-B.

Costa, M. V. C. V. da, Carvalho, O. L. F. de, Orlandi, A. G., Hirata, I., Albuquerque, A. O. de, Silva, F. V. e, Guimarães, R. F., Gomes, R. A. T., and Júnior, O. A. de C. (2021). "Remote Sensing for Monitoring Photovoltaic Solar Plants in Brazil Using Deep Semantic Segmentation." *Energies* 14(10): 2960. doi:https://doi.org/10.3390/en14102960.

Dalponte, M., Coops, N. C., Bruzzone, L., and Gianelle, D. (2009). "Analysis on the Use of Multiple Returns LiDAR Data for the Estimation of Tree Stems volume." *IEEE journal of Selected Topics in Applied Earth Observations and Remote sensing* 2(4):310 - 318.

Dalponte, M., Bruzzone, L., and Gianelle, D. (2008). "Fusion of Hyperspectral and LIDAR Remote Sensing Data for Classification of Complex Forest Areas." *IEEE Transactions on Geoscience and Remote Sensing* 46(5), 1416-1427. doi:https://do i.org/10.1109/TGRS.2008.916480.

Deur, M., Gašparović, M., and Balenović, I. (2021). "An Evaluation of Pixel- and Object-Based Tree Species Classification in Mixed Deciduous Forests Using

Pansharpened Very High Spatial Resolution Satellite Imagery." *Remote Sensing* 1 3(10): 1868. doi:https://doi.org/10.3390/rs13101868.

Dorigo, W., Lucieer, A., Podobnikar, T., and Čarni, A. (2012). "Mapping invasive Fallopia Japonica by Combined Spectral, Spatial, and Temporal Analysis of Digital Orthophotos." *International Journal of Applied Earth Observation and Geoinformation 19*:185-195. doi:https://doi.org/10.1016/j.jag.2012.05.004.

Drăguţ, L., Csillik, O., Eisank, C., and Tiede, D. (2014). "Automated Parameterisation for Multi-Scale Image Segmentation on Multiple Layers." *ISPRS Journal of Photogrammetry and Remote Sensing* 88:119-127. doi:https://doi.org/10.1016/j.isprsjprs.2013.11.018.

Drăguţ, L., Tiede, D., and Levick, S. R. (2010). "ESP : A Tool to Estimate Scale Parameter for Multiresolution Image Segmentation of Remotely Sensed Data." *International Journal of Geographical Information Science* 24(6): 859-871. doi:https://doi.org/10.1080/13658810903174803.

Early, R., Bradley, B. A., Dukes, J. S., Lawler, J. J., Olden, J. D., Blumenthal, D. M., Gonzalez, P., Grosholz, E. D., Ibañez, I., Miller, L. P., Sorte, C. J. B., and Tatem, A. J. (2016). "Global Threats from Invasive Alien Species in the Twenty-first Century and National Response Capacities." *Nature Communications* 7(1): 12485. doi:https://doi.org/10.1038/ncomms12485.

Escadafal, R., and Huete, A. (1991). "Etude des Propriétés Spectrales des Sols Arides Appliquée à l'Amélioration des Indices de Végétation Obtenus par Télédétection." *Comptes rendus de l'Académie des sciences. Série 2, Mécanique, Physique, Chimie, Sciences de l'univers, Sciences de la Terre* 312(11): 1385-1391.

Fernandes, M. R., Aguiar, F. C., Silva, J. M. N., Ferreira, M. T., and Pereira, J. M. C. (2014)." Optimal Attributes for the Object Based Detection of Giant Reed in Riparian Habitats: A Comparative Study Between Airborne High Spatial Resolution and WorldView-2 imagery." *International Journal of Applied Earth Observation and Geoinformation 32*: 79-91. doi:https://doi.org/10.1016/j.jag.2014.03.026.

Frapier, B. (2004). "Experimental Removal of the Non-indigenous Shrub Hhamnus franfiula (Glossy Buckthorn): Effects on Native Herbs and Woody

Seedling's."Northeastern Naturalist 11(3): 333 - 342.doi:https://doi.org/10.1656/1092 - 6194(2004)011[0333:EROTNS]2.0.CO;2.

Gitelson, A. A., Kaufman, Y. J., Stark, R., and Rundquist, D. (2002). "Novel Algorithms for Remote Estimation of Vegetation Fraction." *Remote Sensing of Environment 80*(1): 76-87. doi:https://doi.org/10.1016/S0034-4257(01)00289-9.

Grizonnet, M., Michel, J., Poughon, V., Inglada, J., Savinaud, M., and Cresson, R. (2017) "Orfeo ToolBox : Open Source Processing of Remote Sensing Images." *Open Geospatial Data, Software and Standards* 2(1), 15. doi:https://doi.org/10.1186/s40965-017-0031-6.

Guenther, N., and Schonlau, M. (2016). "Support Vector Machines." *The Stata Journal: Promoting Communications on Statistics and Stata* 16(4): 917-937. https://doi.org/10.1177/1536867X1601600407.

Guido, A., and Pillar, V. D. (2017). "Invasive Plant Removal: Assessing Community Impact and Recovery from Invasion."*Journal of Applied Ecology* 54(4): 1230-1237. doi:https://doi.org/10.1111/1365-2664.12848.

Guyon, I., Weston, J., and Barnhill, S. (2002). "Gene Selection for Cancer Classification Using Support Vector Machines." *Machine Learning*, 34. doi:https://doi.org/10.1023/A:1012487302797

Haralick, R. M. (1979). Statistical and Structural Approaches to Texture. *Proceedings of the IEEE 67*(5), 786-804. doi:https://doi.org/10.1109/PROC.1979.11328

Harrington, R. A., Brown, B. J., and Reich, P. B. (1989). "Ecophysiology of Exotic and Native Shrubs in Southern Wisconsin : I. Relationship of Leaf Characteristics, Resource Availability, and Phenology to Seasonal Patterns of Carbon Gain." *Oecologia 80*(3), 356-367. doi:https://doi.org/10.1007/BF00379037

Heneghan, L., Fatemi, F., Umek, L., Grady, K., Fagen, K., and Workman, M. (2006). "The Invasive Shrub European Buckthorn (Rhamnus cathartica, L.) Alters Soil Properties in Midwestern U.S. woodlands." *Applied Soil Ecology 32*(1), 142-148. doi:https://doi.org/10.1016/j.apsoil.2005.03.009

Jones, D., Pike, S., Thomas, M., and Murphy, D. (2011). "Object-Based Image Analysis for Detection of Japanese Knotweed s.l. Taxa (Polygonaceae) in Wales (UK)." *Remote Sensing 3*(2), 319-342. doi:https://doi.org/10.3390/rs3020319

Kalkman, J. R., Simonton, P., and Dornbos, D. L. (2019). "Physiological Competitiveness of Common and Glossy Buckthorn Compared with Native Woody Shrubs in Forest Edge and Understory Habitats." *Forest Ecology and Management 445*, 60-69. doi:https://doi.org/10.1016/j.foreco.2019.05.007

Knight, K. S., Kurylo, J. S., Endress, A. G., Stewart, J. R., and Reich, P. B. (2007). "Ecology and Ecosystem Impacts of Common Buckthorn (Rhamnus cathartica) : A review." *Biological Invasions 9*(8), 925-937. doi:https://doi.org/10.1007/s10530-007-9091-3

Kumar Rai, P., and Singh, J. S. (2020). "Invasive Alien Plant Species : Their Impact on Environment, Ecosystem Services and Human Health. *Ecological Indicators*, *111*, 106020.

Labonté, J., Drolet, G., Sylvain, J.-D., Thiffault, N., Hébert, F., and Girard, F. (2020). Phenology-Based Mapping of an Alien Invasive Species Using Time Series of Multispectral Satellite Data : A Case-Study with Glossy Buckthorn in Québec, Canada. *Remote Sensing 12*(6), 922. doi:https://doi.org/10.3390/rs12060922

Langmaier, M., and Lapin, K. (2020). "A Systematic Review of the Impact of Invasive Alien Plants on Forest Regeneration in European Temperate Forests." *Frontiers in Plant Science 11*, 524969. doi:https://doi.org/10.3389/fpls.2020.524969

Lavoie, C., Guay, G., and Joerin, F. (2014). "Une Liste des Plantes Vasculaires Exotiques Nuisibles du Québec : Nouvelle Approche pour la Sélection des Espèces et l'Aide à la Décision." *Écoscience 21*(2), 133-156. doi:https://doi.org/10.2980/21-2-3703

Lawrence, R. L., Wood, S. D., and Sheley, R. L. (2006) "Mapping Invasive Plants Using Hyperspectral Imagery and Breiman Cutler Classifications (RandomForest)." *Remote Sensing of Environment 100*(3), 356-362.

Lourenço, P., Teodoro, A. C., Gonçalves, J. A., Honrado, J. P., Cunha, M., and Sillero, N. (2021). "Assessing the Performance of Different OBIA Software Approaches for Mapping Invasive Alien Plants Along Roads with Remote Sensing Data." *International Journal of Applied Earth Observation and Geoinformation 95*, 102263. doi:https://doi.org/10.1016/j.jag.2020.102263

Mack, R. N., Simberloff, D., Mark Lonsdale, W., Evans, H., Clout, M., and Bazzaz, F. A. (2000). "Biotic Invasions : Causes, Epidemiology, Global Consequences, and

Control. *Ecological applications 10*(3), 689-710." doi:Https://doi.org/10.1890/1051-0761 (2000)010[0689:bicegc]2.0.co;2

Mhangara, P., Mapurisa, W., and Mudau, N. (2020). "Comparison of Image Fusion Techniques Using Satellite Pour l'Observation de la Terre (SPOT) 6 Satellite Imagery." *Applied Sciences 10*(5), 1881. doi:https://doi.org/10.3390/app10051881

Müllerová, J., Pergl, J., and Pyšek, P. (2013). "Remote Sensing as a Tool for Monitoring Plant Invasions : Testing the Effects of Data Resolution and Image Classification Approach on the Detection of a Model Plant Species Heracleum Mantegazzianum (Giant Hogweed)." *International Journal of Applied Earth Observation and Geoinformation 25*, 55-65.

Ørka, H. O., Næsset, E., and Bollandsås, O. M. (2009). "Classifying Species of Individual Trees by Intensity and Structure Features Derived from Airborne Laser Scanner Data." *Remote Sensing of Environment 113*(6), 1163-1174. doi:https://doi.org/10.1016/j.rse.2009.02.002

Paz-Kagan, T., Silver, M., Panov, N., and Karnieli, A. (2019). "Multispectral Approach for Identifying Invasive Plant Species Based on Flowering Phenology Characteristics." *Remote Sensing 11*(8), 953. doi:https://doi.org/10.3390/rs11080953

R Core Team (2021). "A Language and Environment for Statistical Computing. R Foundation for Statistical Computing, Vienna, Austria." URL https://www.R-project.org/.

Samat, A., Li, E., Wang, W., Liu, S., Lin, C., and Abuduwaili, J. (2020). "Meta-XGBoost for Hyperspectral Image Classification Using Extended MSER-Guided Morphological Profiles." *Remote Sensing 12*(12), 1973. doi:https://doi.org/10.3390/rs12121973

Shi, Y., Wang, T., Skidmore, A. K., and Heurich, M. (2018). "Important LiDAR Metrics for Discriminating Forest Tree Species in Central Europe." *ISPRS Journal of Photogrammetry and Remote Sensing 137*, 163-174. doi:https://doi.org/10.1016/j.isprsjprs.2018.02.002

Varin, M., Chalghaf, B., and Joanisse, G. (2020). "Object-Based Approach Using Very High Spatial Resolution 16-Band WorldView-3 and LiDAR Data for Tree Species Classification in a Broadleaf Forest in Quebec, Canada." *Remote Sensing 12*(18), 3092. doi:https://doi.org/10.3390/rs12183092

Varin, M, Allostry, J. and Chalghaf, B. 2020. "Caractérisation et Suivi des Écosystèmes Riverains de l'agglomération de Québec - Volet 1 Caractérisation des Écosystèmes Riverains. Centre d'Enseignement et de Recherche en Foresterie de Sainte-Foy inc. (CERFO)." Rapport 2019-14. 24 pages.

Vilà, M., Basnou, C., Pyšek, P., Josefsson, M., Genovesi, P., Gollasch, S., Nentwig, W., Olenin, S., Roques, A., Roy, D., and Hulme, P. E. (2010). "How Well do we Understand the Impacts of Alien Species on Ecosystem Services? A Pan-European, Cross-Taxa Assessment." *Frontiers in Ecology and the Environment 8*(3), 135-144. doi:https://doi.org/10.1890/080083

Waser, L., Küchler, M., Jütte, K., and Stampfer, T. (2014). "Evaluating the Potential of WorldView-2 Data to Classify Tree Species and Different Levels of Ash Mortality." *Remote Sensing 6*(5), 4515-4545. doi:https://doi.org/10.3390/rs60545 15

Yang, L., Mansaray, L., Huang, J., and Wang, L. (2019). "Optimal Segmentation Scale Parameter, Feature Subset and Classification Algorithm for Geographic Object-Based Crop Recognition Using Multisource Satellite Imagery." *Remote Sensing 11*(5), 514. doi:https://doi.org/10.3390/rs11050514

Yang, Y. (2001). "A Study of Thresholding Strategies for Text Categorization. *Proceedings of the 24th Annual International ACM SIGIR Conference on Research and Development in Information Retrieval - SIGIR 01*, 137-145." doi:https://doi.org/10.1145/383952.383975

Zarei, A., Hasanlou, M., and Mahdianpari, M. (2021). "A Comparison of Machine Learning Models for Soil Salinity Estimation Using Multi-Spectral Earth Observation Data." *ISPRS Annals of the Photogrammetry, Remote Sensing and Spatial Information Sciences V-3-2021*, 257-263. doi:https://doi.org/10.5194/isprs-annals-V-3-2021-257-2021

Zhou, Y., Zhang, R., Wang, S., and Wang, F. (2018). "Feature Selection Method Based on High-Resolution Remote Sensing Images and the Effect of Sensitive Features on Classification Accuracy. *Sensors 18*(7), 2013." doi:https://doi.org/10.3390/s18072013

Zhou, Q., Zhang, X., Yu, L., Ren, L., and Luo, Y. (2021). "Combining WV-2 Images and Tree Physiological Factors to Detect Damage Stages of Populus Gansuensis by Asian longhorned beetle (Anoplophora Glabripennis) at the Tree Level." *Forest Ecosystems* 8(1), 1-12.

6. Discussion générale

Ce projet, dont l'objectif principal était de mettre en place une méthode de cartographie des principales EEEv dans un milieu urbain hautement diversifié, a permis de réaliser une classification multi-espèces d'EEEv selon une approche multi-date, avec de bonnes performances pour la renouée du Japon, la berce du Caucase et le phragmite. Les résultats obtenus pour les nerpruns sont également prometteurs et nécessitent d'être améliorées en intégrant d'autres sources de données telles que le LiDAR.

La classification multi-date s'est avérée moins pertinente par rapport à la classification mono-date pour la berce du Caucase et la renouée du Japon. Ainsi, une seule image mono-date à très haute résolution spatiale (WV-3) pourrait permettre de cartographier ces deux EEEv avec une bonne précision dans un contexte similaire au nôtre, à condition que l'image soit acquise durant la période optimale (Juillet-Août). Pour le phragmite, la période d'acquisition des images WV-3 moins optimale n'a pas pu permettre d'atteindre les bonnes performances obtenues pour la berce du Caucase et la renouée du Japon. L'approche multi-date s'est par contre avérée intéressante pour cette espèce. D'autres études antérieures ont également démontré que l'utilisation des données multi-date améliore les performances des modèles de classification pour cette espèce (Rupasinghe et Chow-Fraser, 2019; Abeysinghe *et al*., 2019; Poulin *et al*., 2010). Dans notre étude, l'approche multi-date a donc été privilégiée par rapport à l'approche mono-date, parce que l'objectif était de réaliser une classification simultanée de plusieurs EEEv, caractérisées par des périodes phénologiques de séparabilité optimale différentes. Dans un contexte de ressources financières limitées, l'approche mono-date serait à privilégier.

Afin de réduire les coûts d'acquisition des images multi-date à très haute résolution spatiale, d'autres études sont nécessaires afin d'analyser les performances de cartographie d'EEEv dans des milieux semblables à notre zone d'étude en utilisant des images plus accessibles (gratuites) à moyenne résolution spatiale et acquises en périodes optimales (p. ex. Sentinel-2, Landsat, Planetscope). Cependant, les colonies à détecter doivent être suffisamment développées pour que leur taille soit supérieure ou égale à celle du pixel des images afin d'éviter le problème de mixage spectral (Wang *et al.,* 2022). Pour les détections précoces d'EEEv (colonies moins développées) à partir d'images gratuites à moyenne résolution spatiale, les techniques d'amélioration de la résolution spatiale telle que la super-

résolution peuvent notamment être utilisées (Wang *et al*., 2022; Bachir *et al.,* 2021; Chen *et al*., 2020). Dans notre étude, cette technique a été testée pour le phragmite en utilisant la fusion entre les images Sentinel-2 (10 m) et Planetscope (3 m) acquises en périodes de floraison (Août 2020) et entre SPOT-7 et GeoEye-1 (automne 2020). Les performances étaient médiocres par rapport aux autres approches précédemment présentées (Kappa < 0.5). Nous supposons que le petit nombre d'échantillons, la faible densité des colonies ainsi que la période d'acquisition non optimale (pour l'image SPOT-7) seraient à l'origine de ce résultat obtenu. Afin de réduire les impacts liés aux faibles quantités de données de référence sur les performances de classification, l'utilisation d'algorithmes de classification moins sensibles ou d'autres techniques de sur-échantillonnage des classes minoritaires ou de sous-échantillonnage de la classe majoritaire pourra être envisagée. Des outils de partage des données de référence tels que la plateforme SENTINELLE seraient également une autre alternative permettant l'accès à ces données de référence d'EEEv. Cependant, ces données sont souvent moins précises et une validation de présence pourrait d'abord être réalisée avant leur utilisation (p. ex photo-interprétation).

Pour les nerpruns, d'après les observations réalisées sur terrain, les deux espèces étudiées sont rarement dominantes et se trouvent toujours sous la canopée des autres feuillus dans les endroits colonisés. Cette distribution spatiale des nerpruns explique probablement en grande partie les erreurs de classification observées car les branches et les troncs des autres arbres en surplomb contribueraient fortement à la réflectance des pixels (Labonté *et al.;* 2020), ce qui réduirait la séparabilité avec d'autres espèces. L'utilisation dans un contexte opérationnel (p. ex. : cibler des zones d'intervention) de l'approche développée dans cette étude nécessiterait des améliorations afin de réduire les erreurs de classification obtenues et ainsi cartographier plus précisément les secteurs problématiques. Les prochaines études pourraient notamment intégrer des données LiDAR aux images multispectrales à résolution centimétrique (p. ex. images acquises par drone) afin d'améliorer leur détection sous la couverture forestière. Il n'existe pas, à nos connaissances, de travaux dans la littérature qui ont utilisé les données LiDAR pour cartographier les nerpruns.

7. Conclusion générale

La méthodologie utilisée dans cette étude a permis d'atteindre les objectifs de cartographie multi-espèces d'EEEv et la cartographie des nerpruns sous couverts. La valeur de Kappa obtenue pour le premier objectif est satisfaisante (0.85) et celle obtenue pour le deuxième objectif (0.73) est supérieure à celle obtenue dans d'autres études réalisées dans des conditions complexes similaires à notre zone d'étude, et comparable à celle obtenue dans les études réalisées dans des conditions favorables. Ainsi, les résultats obtenus dans cette étude sont satisfaisants et la méthodologie proposée est également reproductible. Ces résultats démontrent donc la possibilité de réaliser un suivi par télédétection des principales EEEv problématiques dans l'agglomération de Québec à partir d'images satellites THR multi-dates. Les principales limites de ce projet concernent la faible quantité de données de référence d'EEEv, les coûts élevés d'acquisition des images satellitaires multi-dates à très haute résolution spatiale, la faible disponibilité de ces images durant les périodes phénologiques optimales de séparabilité et la distribution des nerpruns en sous-couvert dans notre zone d'étude. Certaines de ces limites, en particulier celles liées à la qualité des données de référence, réduisent les performances de détection de ces EEEv par imagerie multispectrale optique, ce qui nécessite de choisir des modèles d'apprentissage automatique adaptés.

Les probabilités d'appartenance produites dans ce travail par le modèle de prédiction plus performant (RF) peuvent donc servir à la planification des projets et activités de suivi et de contrôle des différentes EEEv qui s'étendent dans certains milieux de la zone d'étude.

8. Références

Abeysinghe, T., Simic Milas, A., Arend, K., Hohman, B., Reil, P., Gregory, A. et Vázquez-Ortega, A. (2019) Mapping Invasive Phragmites australis in the Old Woman Creek Estuary Using UAV Remote Sensing and Machine Learning Classifiers. Remote Sensing, vol. 11, n°11, p.1380.

Agence canadienne d'inspection des aliments (2008) Plantes exotiques envahissantes au Canada, rapport technique, Québec, 20 p.

Abutaleb, K., Newete, S. W., Mangwanya, S., Adam, E. et Byrne, M. J. (2020) Mapping eucalypts trees using high resolution multispectral images: A study comparing WorldView 2 vs. SPOT 7. The Egyptian Journal of Remote Sensing and Space Science, vol. 24, n°3, p. 333-342.

Asner, G. P., Knapp, D. E., Kennedy-Bowdoin, T., Jones, M. O., Martin, R. E., Boardman, J. et Hughes, R. F. (2008) Invasive species detection in Hawaiian rainforests using airborne imaging spectroscopy and LiDAR. Remote Sensing of Environment, vol. 112, n°5, p. 1942-1955.

Bashir S. M. A., Wang Y., Khan M., Niu Y. (2021) A comprehensive review of deep learning-based single image super-resolution. PeerJ Computer Science, 7, p. e621.

Becker, R. H., Zmijewski, K. A. et Crail, T. (2013) Seeing the forest for the invasives: Mapping buckthorn in the Oak Openings. Biological Invasions, vol. 15, n°2, p. 315-326.

Boettcher, T. J., Gautam, S. et Cook, J. (2021) The impact of invasive buckthorn on ecosystem services and its potential for bioenergy production: A Review. Journal of Sustainable Forestry, p.1-23.

Bradley, B. A. (2014) Remote detection of invasive plants: A review of spectral, textural and phenological approaches. Biological Invasions, vol. 16, n°7, p. 1411-1425.

Breiman, L. (2001) Random forests. Machine learning, vol. 45, n°1, p. 5-32.

Carlier, J., Davis, E., Ruas, S., Byrne, D., Caffrey, J. M., Coughlan, N. E., Dick, J. T. A. et Lucy, F. E. (2020) Using open-source software and digital imagery to efficiently and objectively quantify cover density of an invasive alien plant species. Journal of Environmental Management, vol. 266, p. 110519.

Casady, G. M., Hanley, R. S. et Seelan, S. K. (2005) Detection of Leafy Spurge (Euphorbia esula) Using Multidate High-Resolution Satellite Imagery. Weed Technology, vol. 19, n°2, p. 462-467.

Chen M., Ke Y., Bai J., Li P., Lyu M., Gong Z. et Zhou, D. (2020) Monitoring early stage invasion of exotic Spartina alterniflora using deep-learning super-resolution techniques based on multisource high-resolution satellite imagery: A case study in the Yellow River Delta, China. International Journal of Applied Earth Observation and Geoinformation, vol. 92, p. 102180.

Chen, G., Zhao, K. et Powers, R. (2014) Assessment of the image misregistration effects on object-based change detection. ISPRS Journal of Photogrammetry and Remote Sensing, vol. 87, p. 19-27.

Colautti, R. I. et MacIsaac, H. J. (2004) A neutral terminology to define 'invasive' species: Defining invasive species. Diversity and Distributions, vol. 10, n°2, p. 135-141.

Colleran, B., Lacy, S. N. et Retamal, M. R. (2020) Invasive Japanese knotweed (Reynoutria japonica Houtt.) and related knotweeds as catalysts for streambank erosion. River Research and Applications, vol. 36, n°9, p. 1962-1969.

Dash, J. P., Watt, M. S., Paul, T. S. H., Morgenroth, J. et Pearse, G. D. (2019) Early Detection of Invasive Exotic Trees Using UAV and Manned Aircraft Multispectral and LiDAR Data. Remote Sensing, vol. 11, n°15, p. 1812.

Davies, K. W. et Johnson, D. D. (2011) Are We "Missing the Boat" on Preventing the Spread of Invasive Plants in Rangelands? Invasive Plant Science and Management, vol. 4, n°1, p. 166-171.

Dorigo, W., Lucieer, A., Podobnikar, T. et Čarni, A. (2012) Mapping invasive Fallopia japonica by combined spectral, spatial et temporal analysis of digital orthophotos. International Journal of Applied Earth Observation and Geoinformation, vol. 19, p. 185-195.

Early, R., Bradley, B. A., Dukes, J. S., Lawler, J. J., Olden, J. D., Blumenthal, D. M., Gonzalez, P., Grosholz, E. D., Ibañez, I., Miller, L. P., Sorte, C. J. B. et Tatem, A. J. (2016) Global threats from invasive alien species in the twenty-first century and national response capacities. Nature Communications, vol. 7, n°1, 12485.

Environnement Canada (2004) Stratégie nationale sur les espèces exotiques envahissantes. Environnement et Changement climatique, Canada, Québec, 46 p.

Ewald, M., Skowronek, S., Aerts, R., Lenoir, J., Feilhauer, H., Van De Kerchove, R., Honnay, O., Somers, B., Garzón-López, C. X., Rocchini, D. et Schmidtlein, S. (2020) Assessing the impact of an invasive bryophyte on plant species richness using high resolution imaging spectroscopy. Ecological Indicators, vol. 110, p. 105882.

Fernandes, M. R., Aguiar, F. C., Silva, J. M. N., Ferreira, M. T. et Pereira, J. M. C. (2014) Optimal attributes for the object-based detection of giant reed in riparian habitats: A comparative study between Airborne High Spatial Resolution and WorldView-2 imagery. International Journal of Applied Earth Observation and Geoinformation, vol. 32, p. 79-91.

Franklin, S. E., Hall, R. J., Moskal, L. M., Maudie, A. J. et Lavigne, M. B. (2000) Incorporating texture into classification of forest species composition from airborne multispectral images. International Journal of Remote Sensing, vol. 21, n°1, p. 61-79.

Gbedomon, R. C., Salako, V. K. et Schlaepfer, M. A. (2020) Diverse views among scientists on non-native species. NeoBiota, vol. 54, p. 49-69.

Guido, A. et Pillar, V. D. (2017) Invasive plant removal: Assessing community impact and recovery from invasion. Journal of Applied Ecology, vol. 54, n°4, p. 1230-1237.

Hantson, W., Kooistra, L. et Slim, P. A. (2012) Mapping invasive woody species in coastal dunes in the Netherlands: A remote sensing approach using LIDAR and high-resolution aerial photographs. Applied Vegetation Science, vol. 15, n°4, p. 536-547.

Haralick, R. M. (1979) Statistical and structural approaches to texture. Proceedings of the IEEE, vol. 67, n°5, p. 786-804.

Hirayama, H., Sharma, R. C., Tomita, M. et Hara, K. (2019) Evaluating multiple classifier system for the reduction of salt-and-pepper noise in the classification of very-high-resolution satellite images. International Journal of Remote Sensing, vol. 40, n°7, p. 2542-2557.

Hussner, A., Stiers, I., Verhofstad, M. J. J. M., Bakker, E. S., Grutters, B. M. C., Haury, J., van Valkenburg, J. L. C. H., Brundu, G., Newman, J., Clayton, J. S. eterson, L. W. J. et Hofstra, D. (2017) Management and control methods of invasive alien freshwater aquatic plants: A review. Aquatic Botany, vol. 136, p. 112-137.

Ishii, J. et Washitani, I. (2013) Early detection of the invasive alien plant Solidago altissima in moist tall grassland using hyperspectral imagery. International Journal of Remote Sensing, vol. 34, n°16, p. 5926-5936.

IUCN Council (2000) Guidelines for the Prevention of Biodiversity Loss Caused by Alien Invasive Species. in Prepared by IUCN SSC Invasive Species Specialist Group (ISSG) Approved by 51st Meeting IUCN Council Gland Switzerland, p. 12–25.

James, M., Salakpi, E. E., Ouko, E., Yi, Z. F., Antonarakis, A. S., et Rowhani, P. (2021) Mapping Opuntia stricta in the arid and semi-arid environment of kenya using sentinel-2 imagery and ensemble machine learning classifiers. Remote Sensing, vol. 13, n° 8, p. 1494.

Jensen, T., Seerup Hass, F., Seam Akbar, M., Holm Petersen, P. et Jokar Arsanjani, J. (2020) Employing Machine Learning for Detection of Invasive Species using Sentinel-2 and AVIRIS Data: The Case of Kudzu in the United States. Sustainability, vol. 12, n°9, p. 3544.

Jones, D., Pike, S., Thomas, M. et Murphy, D. (2011) Object-Based Image Analysis for Detection of Japanese Knotweed s.l. Taxa (Polygonaceae) in Wales (UK) Remote Sensing, vol. 3, n°2, p. 319-342.

Kalkman, J. R., Simonton, P. et Dornbos, D. L. (2019) Physiological competitiveness of common and glossy buckthorn compared with native woody shrubs in forest edge and understory habitats. Forest Ecology and Management, vol. 445, p. 60-69.

Kattenborn, T., Lopatin, J., Förster, M., Braun, A. C. et Fassnacht, F. E. (2019) UAV data as alternative to field sampling to map woody invasive species based on combined Sentinel-1 and Sentinel-2 data. Remote Sensing of Environment, vol. 227, p. 61-73.

Kavzoglu, T. et Mather, P. M. (2004) The use of backpropagating artificial neural networks in land cover classification. International journal of remote sensing, vol. 24, n°23, p. 4907-4938

Kelsch, A., Takahashi, Y., Dasgupta, R., Mader, A. D., Johnson, B. A. et Kumar, P. (2020) Invasive alien species and local communities in socio-ecological production landscapes and seascapes: A systematic review and analysis. Environmental Science and Policy, vol. 112, p. 275-281.

Kganyago, M., Odindi, J., Adjorlolo, C. et Mhangara, P. (2018) Evaluating the capability of Landsat 8 OLI and SPOT 6 for discriminating invasive alien species in the African Savanna landscape. International Journal of Applied Earth Observation and Geoinformation, vol. 67, p. 10-19.

Kumar Rai, P. et Singh, J. S. (2020) Invasive alien plant species: Their impact on environment, ecosystem services and human health. Ecological Indicators, vol. 111, p. 106020.

Labonté, J., Drolet, G., Sylvain, J.-D., Thiffault, N., Hébert, F. et Girard, F. (2020) Phenology-Based Mapping of an Alien Invasive Species Using Time Series of Multispectral Satellite Data: A Case-Study with Glossy Buckthorn in Québec, Canada. Remote Sensing, vol. 12, n°6, p. 922.

Langmaier, M. et Lapin, K. (2020) A Systematic Review of the Impact of Invasive Alien Plants on Forest Regeneration in European Temperate Forests. Frontiers in Plant Science, vol. 11, p. 1349.

Lantz, N. J. et Wang, J. (2013) Object-based classification of Worldview-2 imagery for mapping invasive common reed, Phragmites australis. Canadian Journal of Remote Sensing, vol. 39, n°4, p. 328-340.

Lass, L. W., Prather, T. S., Glenn, N. F., Weber, K. T., Mundt, J. T. et Pettingill, J. (2005) A review of remote sensing of invasive weeds and example of the early detection of spotted knapweed (Centaurea maculosa) and babysbreath (Gypsophila paniculata) with a hyperspectral sensor. Weed Science, vol. 53, n°2, p. 242-251.

Lavoie, C., Guay, G. et Joerin, F. (2014) Une liste des plantes vasculaires exotiques nuisibles du Québec : Nouvelle approche pour la sélection des espèces et l'aide à la décision. Écoscience, vol. 21, n°2, p. 133-156.

Lawrence, R., Hurst, R., Weaver, T. et Aspinall, R. (2006) Mapping Prairie Pothole Communities with Multitemporal Ikonos Satellite Imagery. Photogrammetric Engineering and Remote Sensing, vol. 72, n°2, p. 169-174.

Lawrence, R. L., Wood, S. D. et Sheley, R. L. (2006) Mapping invasive plants using hyperspectral imagery and Breiman Cutler classifications (randomForest), Remote Sensing of Environment, vol. 100, n°3, p. 356-362.

Lee, S. (2018) Editorial for Special Issue: “Application of Artificial Neural Networks in Geoinformatics”. Applied Sciences, vol. 8, n°1, p. 55.

Lu, D. et Weng, Q. (2007) A survey of image classification methods and techniques for improving classification performance. International Journal of Remote Sensing, vol. 28, n°5, p. 823-870.

Martin, F.-M., Müllerová, J., Borgniet, L., Dommanget, F., Breton, V. et Evette, A. (2018) Using single- and multi-date UAV and satellite imagery to accurately monitor invasive knotweed species. Remote Sensing, vol. 10, n°10, p. 1662.

Martínez-Izquierdo, L., García, M. M., Powers, J. S. et Schnitzer, S. A. (2016) Lianas suppress seedling growth and survival of 14 tree species in a Panamanian tropical forest. Ecology, vol. 97, n°1, p. 215-224.

Martínez-Sánchez, J., González-de Santos, L. M., Novo, A. et González-Jorge, H. (2019) UAV and satellite imagery applied to alien species mapping in nw spain. ISPRS - International Archives of the Photogrammetry, Remote Sensing and Spatial Information Sciences, XLII-2/W13, p. 455-459.

Marvin, D. C., Asner, G. P. et Schnitzer, S. A. (2016) Liana canopy cover mapped throughout a tropical forest with high-fidelity imaging spectroscopy. Remote Sensing of Environment, vol. 176, p. 98-106.

Masse, A. (2013) Développement et automatisation de méthodes de classification à partir de séries temporelles d’images de télédétection - Application aux changements d'occupation des sols et à l'estimation du bilan carbone. Thèse de doctorat, Université Toulouse III Paul Sabatier, Toulouse, 190 p.

Ministère de l’Environnement et de la Lutte contre les Changements climatique (MELCC) (2020) Sentinelle, Outil de détection des espèces exotiques envahissantes. site web: http://www.environnement.gouv.qc.ca/biodiversite/especes- exotiques envahissan tes/sentinelle.html (consulté le 10 octobre 2020)

Michez, A., Piégay, H., Jonathan, L., Claessens, H., & Lejeune, P. (2016). Mapping of riparian invasive species with supervised classification of Unmanned Aerial

System (UAS) imagery. International Journal of Applied Earth Observation and Geoinformation, vol. 44, p. 88-94.

Müllerová, J., Bartaloš, T., Brůna, J., Dvořák, P. et Vítková, M. (2017) Unmanned aircraft in nature conservation: An example from plant invasions. International Journal of Remote Sensing, vol. 38, n°8-10, 2177-2198.

Müllerová, J., Pergl, J. et Pyšek, P. (2013) Remote sensing as a tool for monitoring plant invasions: Testing the effects of data resolution and image classification approach on the detection of a model plant species Heracleum mantegazzianum (giant hogweed) International Journal of Applied Earth Observation and Geoinformation, vol. 25, p. 55-65.

Müllerová, J., Pyšek, P., Jarošík, V. et Pergl, J. (2005) Aerial photographs as a tool for assessing the regional dynamics of the invasive plant species Heracleum mantegazzianum: Regional dynamics of H. mantegazzianum invasion. Journal of Applied Ecology, vol. 42, n°6, p. 1042-1053.

Niphadkar, M. (2016) Remote sensing of invasive plants: Incorporating functional traits into the picture. International journal of remote sensing, 13.

Noble, W. S. (2006) What is a support vector machine? Nature Biotechnology, vol. 24, n° 12, p. 1565-1567.

Paz-Kagan, T., Silver, M., Panov, N. et Karnieli, A. (2019) Multispectral Approach for Identifying Invasive Plant Species Based on Flowering Phenology Characteristics. Remote Sensing, vol. 11, n°8, p. 953.

Poulin B., Davranche A. et Lefebvre G. (2010). Ecological assessment of Phragmites australis wetlands using multi-season SPOT-5 scenes. Remote Sensing of Environment, vol.114, n°7, pp. 1602-1609.

Qian, W., Huang, Y., Liu, Q., Fan, W., Sun, Z., Dong, H., Wan, F. et Qiao, X. (2020) UAV and a deep convolutional neural network for monitoring invasive alien plants in the wild. Computers and Electronics in Agriculture, vol. 174, p. 105519.

Rew, L. J. et Cousens, R. D. (2001) Spatial distribution of weeds in arable crops: Are current sampling and analytical methods appropriate? Weed Research, vol. 41, n° 1, p. 1-18.

Richardson, D. M., Pysek, P., Rejmanek, M., Barbour, M. G., Panetta, F. D. et West, C. J. (2000) Naturalization and invasion of alien plants : Concepts and definitions. Diversity and Distributions, vol. 6, n°2, p. 93-107.

Richardson, D. M. et Thuiller, W. (2007) Home away from home—Objective mapping of high-risk source areas for plant introductions. Diversity and Distributions, vol. 13, n°3, p. 299-312.

Rizaludin Mahmud, M., Numata, S. et Hosaka, T. (2020) Mapping an invasive goldenrod of Solidago altissima in urban landscape of Japan using multi-scale remote sensing and knowledge-based classification. Ecological Indicators, vol. 111, p. 105975.

Roy, H. E., Bacher, S., Essl, F., Adriaens, T., Aldridge, D. C., Bishop, J. D. D., Blackburn, T. M., Branquart, E., Brodie, J., Carboneras, C., Cottier-Cook, E. J., Copp, G. H., Dean, H. J., Eilenberg, J., Gallardo, B., Garcia, M., García-Berthou, E., Genovesi, P., Hulme, P. E., … Rabitsch, W. (2019) Developing a list of invasive alien species likely to threaten biodiversity and ecosystems in the European Union. Global Change Biology, vol. 25, n°3, p. 1032-1048.

Royimani, L., Mutanga, O., Odindi, J., Dube, T. et Matongera, T. N. (2019) Advancements in satellite remote sensing for mapping and monitoring of alien invasive plant species (AIPs) Physics and Chemistry of the Earth, Parts A/B/C, vol. 112, p. 237–245.

Rupasinghe P. A. et Chow-Fraser P. (2021) Mapping Phragmites cover using WorldView 2/3 and Sentinel 2 images at Lake Erie Wetlands, Canada. Biological Invasions, vol.23, n°4, pp. 1231-1247.

Sagi, O., et Rokach, L. (2021) Approximating XGBoost with an interpretable decision tree. Information Sciences, 572, p. 522-542.

Samat A., Li E., Wang W., Liu S., Lin C.et Abuduwaili J. (2020) Meta-XGBoost for Hyperspectral Image Classification Using Extended MSER-Guided Morphological Profiles. Remote Sens., 12 (12), p.1973.

Sánchez-Azofeifa, G. A., Castro, K., Wright, S. J., Gamon, J., Kalacska, M., Rivard, B., Schnitzer, S. A. et Feng, J. L. (2009) Differences in leaf traits, leaf internal structure et spectral reflectance between two communities of lianas and trees: Implications

for remote sensing in tropical environments. Remote Sensing of Environment, vol. 113, n°10, p. 2076-2088.

Schnitzer, S. A. (2005) A Mechanistic Explanation for Global Patterns of Liana Abundance and Distribution. The American Naturalist, vol. 166, n°2, p. 262-276.

Shackleton, R. T., Biggs, R., Richardson, D. M. et Larson, B. M. H. (2018) Social-ecological drivers and impacts of invasion-related regime shifts: Consequences for ecosystem services and human wellbeing. Environmental Science and Policy, vol. 89, p. 300-314.

Shendryk, Y., Rossiter-Rachor, N. A., Setterfield, S. A. et Levick, S. R. (2020) Leveraging High-Resolution Satellite Imagery and Gradient Boosting for Invasive Weed Mapping. IEEE Journal of Selected Topics in Applied Earth Observations and Remote Sensing, vol. 13, p. 4443-4450.

Shiferaw, H., Bewket, W. et Eckert, S. (2019) Performances of machine learning algorithms for mapping fractional cover of an invasive plant species in a dryland ecosystem. Ecology and Evolution, vol.9, n°5, p. 2562-2574.

Shine, C. (2007) Invasive species in an international context: IPPC, CBD, European Strategy on Invasive Alien Species and other legal instruments. EPPO Bulletin, vol. 37, n°1, p. 103-113.

Somerville, G. J., Sønderskov, M., Mathiassen, S. K. et Metcalfe, H. (2020) Spatial Modelling of Within-Field Weed Populations, a Review. Agronomy, vol. 10, n° 7, p. 1044.

Ustin, S. L., DiPietro, D., Olmstead, K., Underwood, E. et Scheer, G. J. (2002) Hyperspectral remote sensing for invasive species detection and mapping. IEEE International Geoscience and Remote Sensing Symposium, vol. 3, p. 1658-1660.

Vaz, A. S., Alcaraz-Segura, D., Campos, J. C., Vicente, J. R. et Honrado, J. P. (2018) Managing plant invasions through the lens of remote sensing: A review of progress and the way forward. Science of the Total Environment, vol. 642, p. 1328-1339.

Vilà, M., Espinar, J. L., Hejda, M., Hulme, P. E., Jarošík, V., Maron, J. L., Pergl, J., Schaffner, U., Sun, Y. et Pyšek, P. (2011) Ecological impacts of invasive alien plants: A meta-analysis of their effects on species, communities and ecosystems:

Ecological impacts of invasive alien plants. Ecology Letters, vol. 14, n°7, p. 702-708.

Wang Y., Bashir S. M. A., Khan M., Ullah Q., Wang R.et Song Y., ... ,Niu Y. (2022) Remote sensing image super-resolution and object detection: Benchmark and state of the art. Expert Systems with Applications, p. 116793.

Wilfong, B. N., Gorchov, D. L. et Henry, M. C. (2009) Detecting an Invasive Shrub in Deciduous Forest Understories Using Remote Sensing. Weed Science, vol. 57, n°5, p. 512-520.

Xu, C.-Y., Griffin, K. L. et Schuster, W. S. F. (2007) Leaf phenology and seasonal variation of photosynthesis of invasive Berberis thunbergii (Japanese barberry) and two co-occurring native understory shrubs in a northeastern United States deciduous forest. Oecologia, vol. 154, n°1, p. 11-21.

Young, A. M. et Larson, B. M. H. (2011) Clarifying debates in invasion biology: A survey of invasion biologists. Environmental Research, vol. 111, n°7, p. 893-898. Yu, Q. (2020) Remote Sensing of Potamogeton crispus L. in Dongping Lake in the North China Plain Based on Vegetation Phenology. Journal of the Indian Society of Remote Sensing, vol. 48, n°4, p. 563-573.

Zarei A., Hasanlou M.et Mahdianpari M. (2021) A comparison of machine learning models for soil salinity estimation using multi-spectral earth observation data. ISPRS Ann. Photogramm. Remote Sensing and Spatial Information Sciences, V-3-2021, pp. 257-263.

Zhang, L., Zhang, L. et Du, B. (2016) Deep Learning for Remote Sensing Data: A Technical Tutorial on the State of the Art. IEEE Geoscience and Remote Sensing Magazine, vol. 4, n°2, p. 22-40.

9. Annexes

Annexe 1 : Preuve de soumission de l'article 1

Submission received for GIScience & Remote Sensing (Submission ID: 221156402)

TGRS-peerreview@journals.tandf.co.uk <TGRS-peerreview@journals.tandf.co.uk>
Jeu 2022-08-04 01:34
À : Fiston Nininahazwe <fiston.nininahazwe@usherbrooke.ca>

Dear Fiston Nininahazwe,

Thank you for your submission.

Submission ID	**221156402**
Manuscript Title	**Mapping invasive alien plant species with very high spatial resolution and multi-date satellite imagery using object-based and machine learning techniques: A comparative study**
Journal	**GIScience & Remote Sensing**

You can check the progress of your submission, and make any requested revisions, on the Author Portal.

Thank you for submitting your work to our journal.
If you have any queries, please get in touch with TGRS-peerreview@journals.tandf.co.uk.

Kind Regards,
GIScience & Remote Sensing Editorial Office

Annexe 2 : Preuve de soumission de l'article 2

Submission received for International Journal of Digital Earth (Submission ID: 223911699)

TJDE-peerreview@journals.tandf.co.uk <TJDE-peerreview@journals.tandf.co.uk>
Lun 2022-08-08 20:30
À : Fiston Nininahazwe <fiston.nininahazwe@usherbrooke.ca>

Dear Fiston NININAHAZWE,

Thank you for your submission.

Submission ID	**223911699**
Manuscript Title	**Mapping common and glossy buckthorns (Frangula alnus and Rhamnus cathartica) using multi-date satellite imagery WorldView-3, GeoEye-1 and SPOT-7.**
Journal	**International Journal of Digital Earth**
Article Publishing Charge (APC)	**USD $0.00 (plus VAT or other local taxes where applicable in your country)**

**APC only payable if your article is accepted*

You can check the progress of your submission, and make any requested revisions, on the Author Portal.

Thank you for submitting your work to our journal.
If you have any queries, please get in touch with TJDE-peerreview@journals.tandf.co.uk.

For any queries relating to your APC, please get in touch with APC@tandf.co.uk

Kind Regards,
International Journal of Digital Earth Editorial Office

Annexe 3 : Illustration of fusion results: initial image (a), local mean and variance matching fusion (b), Bayesian fusion (c), Gram-Schmidt fusion (d), ratio component substitution fusion (e), and Zhang fusion (f)